



Analyzing the Impact of Climate Data Using Geospatial Techniques on Land Use and Land Cover Changes in the Kaveri River Basin, Manmangalam Taluk, Karur District, Tamil Nadu

Varunprasath Krishnaraj · Jeevitha Palanisamy

Received: 25 August 2023 / Accepted: 30 January 2024 / Published online: 17 February 2024
© The Author(s), under exclusive licence to Springer Nature Switzerland AG 2024

Abstract Knowledge of variations in climate, changes, and forecasts is critical for improved water utilization and development in a region. Because the water reserves of the Kaveri River basin in Manmangalam Taluk, Karur District, are extremely susceptible to a shifting climate, the current study utilized 31 years of information on climate data, including the earth's surface skin temperature (EST), temperature, and precipitation, and also analyzed human disturbance score (HDS) that impacts land use and land cover shifts. The HDS scores of water bodies are further graded and categorized into low, middle, and high impacts by the method (Gernes & Helgen, 2002) with slight modification. Here is a statistically not significant but positive correlation between the year and earth's skin temperatures ($r = .152$, $N = 27$, $p > .001$). Temperature and year exhibit a substantial, positive link ($r = .255$, $N = 27$, $p > .001$) and were statistically connected. The association between the year and precipitation was non-significant and positive ($r = .064$, $N = 27$, $p > .001$). Also, the relationship between years and human disturbance score levels was shown to be significantly positive ($r = .953$, $N = 27$, $p > .001$). HDS values are classified into three types. The minimum ranges from 34 to 75. The least impacted (LI)

was 7.40% from 1995 to 1997, the most impacted (MI) was 51.85% from 1997 to 2010, and the most impacted (HI) is presently 40.74% because nearby counties gained a substantial number of people following the economic developments, resulting in an abrupt shift in its LULC pattern. Also, the purpose of this investigation is to examine the shifts in LULC from 2004 to 2022 by using QGIS software. The findings reveal major shifts, with a constant increase in urban areas and open/fallow areas and a decline in cropland and vegetation. Throughout the research span, the residential area expanded by 15.24% and open land grew by 3.94%, whereas farming surfaces were reduced. The reduction of agricultural land for cultivation and plant cover has significantly contributed to the growth of built-up areas, while urban sprawl has replaced foliage, ridges, and farms.

Keywords Earth's surface skin temperature · Bhavani River · Soil organic carbon · NDVI · Land cover change · Remote sensing

1 Introduction

Climate change is expected to have a greater impact on biologically relevant river flow characteristics worldwide by the 2050s. The worldwide hydrological cycle has become much more intense over the years as a consequence of economic development, land use/cover variation, and changes in the climate,

V. Krishnaraj (✉) · J. Palanisamy
Department of Zoology, PSG College of Arts
and Science, Civil Aerodrome Post, Coimbatore-14,
Tamil Nadu 641 014, India
e-mail: varunprasath@psgcas.ac.in

impacting water security, health of ecosystems, and river diversity (Van vliet et al., 2013; Fugère et al., 2016). Climate modification is one of the foremost serious intimidations to aquatic life because it causes significant, unpredictable environmental fluctuation (Dudgeon et al., 2006; Woodward et al., 2010). According to Döll and Zhang (2010), inquiries of how future warming might affect flow patterns and aquatic habitats have mostly been carried out at the basin level (Ahn et al., 2018; González-Villela et al., 2018; Thompson et al., 2021) or for smaller individual sites (House et al., 2017; Thompson et al., 2017). The interaction of hydrological and climatological data and analytics provides a mature ability for assessing predicted land water flows. Rainfall and temperatures are two climatic factors that must be investigated to identify their effect on the environment, farming, and humanity (Wang et al., 2016; Yu et al., 2014; Chen et al., 2014; Piao et al., 2014; Karl, 1998). The physical temperature of the earth's surface is known as skin temperature (Ts), as previously clarified by Norman and Becker (1995). It is worth noting that the earth's surface skin temperature is important in predicting future variation in the floor and underneath hydrometeorological, land-atmosphere, and ecological effect examinations, with sunlight assisting as the main motivation (Himika & Kaur, 2018; Endo et al., 2015). Alterations in the atmospheric layers, such as temperature, precipitation, and additional climatic variables, are examples of climate change. Numerous studies have demonstrated the influence of climate change on rainfall and river flow. Morello et al. (2014), Trenberth (2015), and Qin et al. (2018) indicated that the stagnation of temperature global warming and variability in the climate (such as the occurrence of severe storms and the pattern of spatiotemporal temperature shifts) result in the spatial redistribution of watersheds and a spike in the frequency of floods and droughts disasters. River water's physical qualities are affected by climate factors such as air temperature (Mohseni et al., 1999; Webb et al., 2003) and rainfall (Sinokrot & Gulliver, 2000). The environments of freshwater are diverse, commercially significant, and rapidly threatened by human impacts (Dodds et al., 2009; Dudgeon et al., 2006; Pimentel et al., 2005; Vitousek et al., 1997). LULC and soil loss have an adverse effect on the ecology in the stream basin (Setegn et al., 2008; Srinivasan et al., 2010). Increased urbanization and

land use decisions across watersheds frequently produce significant variations in water flow speeds and the quantity of silt carried (Pazúr & Bolliger, 2017). The mining creates additional land uses that change the properties of the soil; it degrades the ecosystem and changes the landscape. It is crucial to map this degradation, particularly if it comes to ecological preservation and studies on changes in the climate (Cetin et al., 2023). Population growth and migration from rural to urban areas have significantly increased urban density, causing numerous problems (Adiguzel et al., 2020, 2022; Bozdogan Sert et al., 2019, 2021; Kilicoglu et al., 2021). LULC alterations are critical for identifying spatiotemporal sustainability because they are strongly linked to regional, national, and global weather ailments: the carbon phase, ecological diversity strength, water quality, sustainable farming, and food availability (Meer & Mishra, 2020; Meshesha et al., 2014). The primary source of organic carbon for terrestrial ecosystems is the soil. According to Korkanç et al. (2018), a decline in soil organic carbon (SOC) weakens ecosystem resilience, biological diversity, and production. Increased urbanization and land use decisions across watersheds frequently produce significant variations in water flow speeds and the quantity of silt carried (Pazúr & Bolliger, 2017). The growth of residential areas globally has led to an increase in environmental issues, particularly pollution. Heavy metals, particularly lead and copper, pose a significant threat to human and environmental health due to their increasing concentration in the environment. Soil, a crucial environment element, is significantly impacted by pollution, providing plants with nourishment and a living environment, while topsoil is a significant indicator of air pollution (Cetin & Jawed, 2022). Wang et al. (2016) denote that noise pollution, bird and bat fatalities, greenhouse gas emissions, and local climate are the most significant environmental impacts of wind power. Landscape engineering impresses the main ideas, concepts, and techniques that cope with the functional, visual, and ecological perspectives of grading and landform cultivation. Air pollution poses a significant threat to human health, particularly in urban areas, with 90% of the global population breathing polluted air, causing approximately 7 million annual deaths (Cesur et al., 2022). Wind power does not cause air pollution or other forms of environmental degradation associated with fossil fuel technologies (Farfan et al., 2009).

Soil organic carbon (SOC) can significantly affect other soil physicochemical properties, water quality (Lal, 2003; Berhe et al., 2014), crop yield (Maia et al., 2010), and climate change (Lal, 2004; Scharlemann et al., 2014). They can also alter humidity, air, and surface temperatures (Armstrong et al., 2016; Rajewski et al., 2020; Xia et al., 2016; Zhou et al., 2012); however, this is not always the case (Moravec et al., 2018). A few researches indicate that wakes might affect the vegetation. Soil is the main material used in the construction of building foundations. In the last 30 years, with the advances in computer technologies, Geographic Information Systems (GIS) are a frequently used tool for storing, processing, and analyzing spatial data (Şimşek et al., 2018). The atmosphere has been overrun by anthropogenic pollutants over the last three to four decades, bringing air quality to a dangerous level that jeopardizes human health (Cetin & Abo Aisha, 2023; Cetin & Jawed, 2021, 2022; Cetin et al., 2023; Shahid et al., 2017). Most of the world's food supply depends on the existence of fertile soils.

One important aspect and result of global environmental change is, in part, a change in land use and land cover (LULC) (Song et al., 2018). Human change of the earth's terrestrial surface from one usage to another is referred to as LULC (Meshesha et al., 2012). Urban climate highlights the significant changes brought about by various climatic elements within the extremely complex built environment of cities. The estimation and detection of the same seasons for different years from LULC maps will be highly beneficial, taking into account the phenological influence and seasonal adaptation (Lu et al., 2019). The LULC matrix is a fundamental part of the surroundings, and it is linked in either way to several financial and geophysical characteristics. The phrases "land cover" and "land use" may be utilized collectively, yet each has distinct meanings (Alawamy et al., 2020). A large number of researchers and academics have also extensively studied changes in land cover/use related to various issues, such as urbanization (Abass et al., 2018; Abrantes et al., 2016; Aduah & Baffoe, 2013; Dong et al., 2008; Tan et al., 2010), agriculture (Baessler & Klotz, 2006; Börjesson & Tufvesson, 2011; Futemma & Brondizio, 2003; Klink et al., 1993; Liu et al., 2004; Walsh et al., 2003), and tourism (Atik et al., 2010; Boavida-Portugal et al., 2016; Dong et al., 2008; Mao et al., 2014; Stankov

et al., 2016; Xi et al., 2014). The impact of a shift in LULC on a stream watershed is directly proportional to the degree of changes occurring to natural land cover caused by human influences, which depends on the force, position, and sort of modification occurring within a catchment (Warburton et al., 2012). Therefore, a small watershed, less than 1 km², replies extra powerfully to land use changes than a large river basin, which is greater than 100 km² due to the many complex processes associated with it (Costa et al., 2003). In a vast river region, distinguishing the influence of LULC shifts in all classes on the hydrological response gets challenging. As a result, the combined impacts of shifts in LULC on river flow are found at the basin's outflow. Multiple variables influence the flow structure of significant river basins around the world, namely changes in land use, world climate variability, water route distractions, and riverside seizures for temporary reserves. By 2025, the effects of changing land cover brought on by increased land use may surpass those of global warming (Vorosmarty et al., 2000). Mapping and quantifying the status of variations in LULC and the variables driving them for those changes is important for assessing the critical areas of change and helps in designing sustainable ecosystem services. To detect land use, setting of baselines with further surveillance is important, as timely information is necessary to figure out the present value of land and its type of usage, which helps to average annual fluctuations in land utilization (Twisa & Buchroithner, 2019). In past decades, LULC's changes have served as the most focused and interesting area of research as these changes affect runoff, sediment yield, evaporation, groundwater recharge, and water yield (DeFries & Eshleman, 2004). In countries with limited water resources and rapid changes in underground use, there are water shortage problems. In different parts of the country, rapid urbanization and development have made massive changes in socioeconomic aspects, and in the future, it is estimated to have further effects (Lambin et al., 2003). Many studies on LULC changes were done in the Karur District (Alaguraja Palanichamy, 2013; Suvetha & Maniyosai, 2018; Balachandar et al., 2011; Ravichandran & Manonmani, 2021). Thirty-one years of prior yearly climate information on earth's surface skin temperature, precipitation, temperature, and human disturbance score were collected from power.larc.nasa.gov and utilized to analyze its

effect on LULC variations in the Kaveri River basin, Karur. Land alterations in the Kaveri River basin are still not being examined systematically, and efforts to determine their scope are unusual. In addition, we use Landsat images from 2004, 2014, and 2022 to map and measure the region's spatiotemporal LULC fluctuations using GIS techniques and QGIS technology.

2 Study Area

Karur District (Lat $10^{\circ} 57' 10.155''$ N, Lon $78^{\circ} 4' 40.031''$ E) is bounded on the north by Namakkal, on the southeast by Dindigul, on the east side by Tiruchirappalli, and on the western side by Erode found in the state of TamilNadu as shown in Figure 1. Karur is located on the banks of the Amaravati River. Due to Karur's rain shade, the southwest monsoon, which starts in June and endures until August, brings minimal rain. The northeast monsoon, which usually comes from October to December, brings most of the rain over summertime (later April and May). The district's geography is generally flat, with the exception of the Rengamalai mountains in the southernmost part of Karur Taluk. Kulithalai Taluk is home to

the Tipasamymalai and Vellimalai hills. The Kaveri River runs across its north and eastern boundaries in the Karur District. The basin has a tropical climate with a median yearly precipitation of 900 mm (Indian Meteriological Department, 2001), 90% of which falls around the southwest monsoon season. It is a key source of water supply for domestic, agricultural, and industrial purposes. Three small rivers, the Palar, the Chennar, and the Thoppar, join the Kaveri as it flows over Stanley reservoir in Mettur and continues into the Erode district, where it unites into the Bhavani River. The surrounding waters have been widely used for manufacturing water usage and disposal of trash, resulting in significant pollution from a huge number of fabric dyeing and bleaching plants, particularly in the Karur area. The district covers 2586 km^2 and has a population of 1,474,646 in 2023 (uidai.gov.in, 2023). Karur is defined by moderate rainfall and forests covering 61.87 km^2 or about 15% of the region's geography median altitude of 101 m (331 ft). The climate is hot and dry during the summer months from March to May, while winter is cold and misty, lasting from November to February. Temperature ranges from a maximum of 102°F and minimum of 39°F (Indian Meteriological Department, 2001). The most

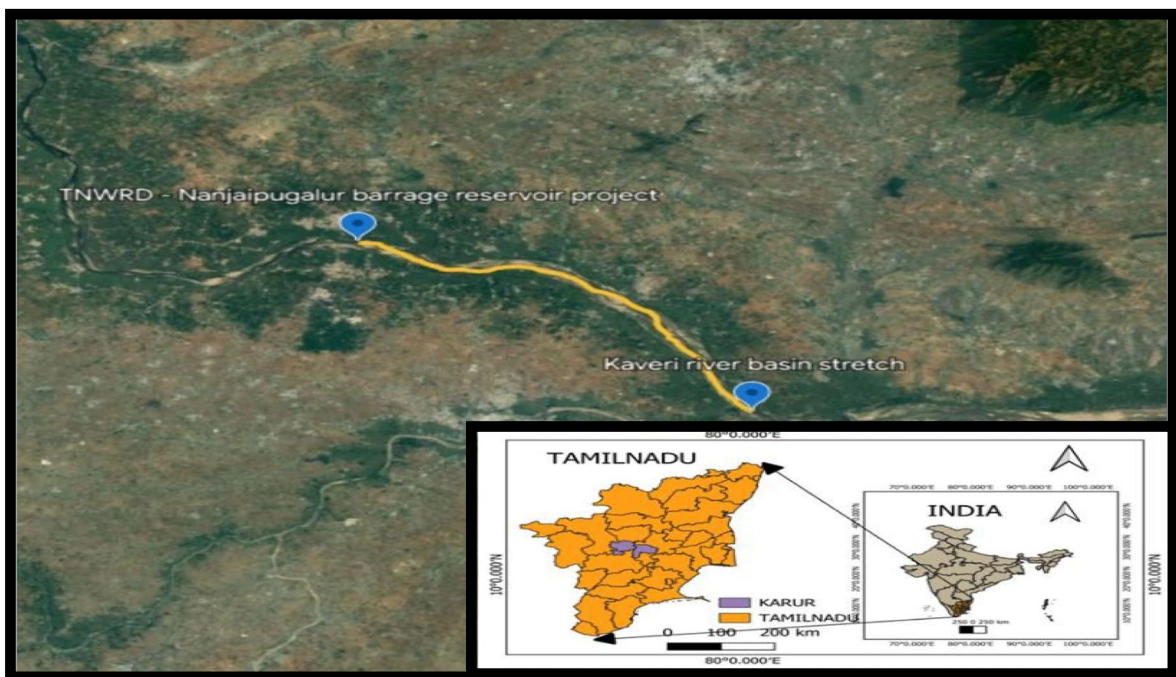


Fig. 1 Study area of Kaveri River, Karur District

commonly grown crops include paddy, sorghum, groundnut, green gram, black gram, maize, cotton, and sugarcane.

Figure 1 represents the actual area of interest.

3 Methodology

We concentrate on the evaluation of LULC identification by cartography for successful environmental, land use, and hydrological regulations in the research area. Bhavani River serves as one of the primary branches of the Bhavai River, which runs into the Manmangalam Taluk, Karur.

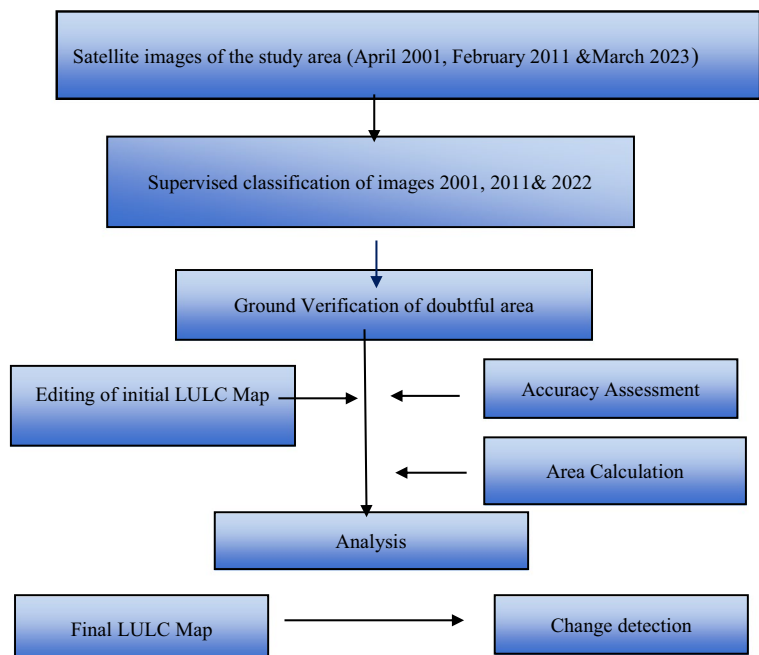
4 LULC Utilization

Landsat images (TM, ETM+, and OLIS/TIRS) attained from the US Geological Survey (USGS, <https://www.usgs.gov/>) were used to examine the LULC of the study region (Mettupalayam Taluk, Coimbatore district). All pictures were reserved between 2014 and 2022 and were cloud-free. In the Manmangalam Taluk, Karur District, QGIS is being utilized to investigate variances in LULC classes. The UGGS provided Landsat 8 thematic mapper

(TM) pictures for 2014 with a pixel firmness of 30–120 m and Landsat 8 in OLI operation land photos with nine spectral bands resolving 114,112 mm for 2022. The photographs were all shot between 2014 and 2022 and were cloud-free (Fig. 2).

Previously, the level 1 bands were evaluated geographically at UTM zone 43N WGS84. For use with the research area border shapefile, the images were combined and removed in QGIS 3.30. Following image improvements (usual distorted layout and standard deviation extension) produced adequate instructive polygons to state LULC types with QGIS 3.30’s training design manager (Lillesand et al., 2015). The five images were classified into five land use subgroups via the variational forest image classification system (water bodies, farming regions, urban areas, and arid lands). Breiman (2001) anticipated unexpected forestry, which experts gradually accepted. This is because it outperforms older picture-sorting techniques and achieves excellent sorting precision when using limited and condensed training information. To estimate the level of diverse LULC variance, the quantity changeability (PC, Eq. (1)) and conversion possibility strategies were utilized (Fenta et al., 2017; Berihun et al., 2019; Gashaw et al., 2018).

Fig. 2 LULC classification methodology



$$PC = \frac{U_a - U_b}{U_a} \times 100,$$

where PC is the LULC rate of change; U_a is the area of start-date LULC type; and U_b is the area of end-date LULC type.

A land use change matrix was utilized to display how the trend and section of several LULC kinds vary over time. This was done via crossover, overlay, and overlap in QGIS3.30 software across various points in time. The attribute stands gained from the revisions were converted to Microsoft Excel in order to subtract the area shift and frequency of variation over time. Execution grouping accuracy valuation (kappa coefficient and overall accuracy) via ground visit, group debate, aerial pictures, interviews with significant informants, and image references corroborated with the precision

$$\text{User accuracy} = \frac{\text{number of correctly classified pixels in each category}}{\text{total number of reference pixels in that category (the row total)}} \times 100,$$

$$\text{Producer accuracy} = \frac{\text{number of correctly classified pixels in each category}}{\text{total number of reference pixels in that category}} \times 100,$$

$$\text{Total (overall) accuracy} = \frac{\text{number of correctly classified pixels in each category}}{\text{total number of reference pixel}} \times 100.$$

output map (Congalton, 1991a, 1991b). Table 1 shows the Manmangalam Taluk LULC classes and their definitions.

In 2023, the image was trained and validated using information gathered from Google Earth, inquiries, and observation trips. For each LULC group, 50 to 60 points for ground truth and Google Earth-Pro photos were attained in the field (Lillesand et al., 2015). Finally, using the QGIS programme, the photos of the five LULC classifications, specifically lakes and rivers, forests, farmland, built-up regions, and barren land, were categorized. All pictures filled the space between the Manmangalam Taluk. Raster images were used to distinguish the several study regions by the clip raster by mask layer in the Raster extraction tool present in the processing toolbox. The spread of area statistics is shown together with LULC images in Fig. 8 and Table 1 respectively.

5 Meteorological Data

For our study area, River Kaveri, Karur, we used meteorological data from the forecast of Worldwide Energy Resources (POWER) 2003 (power.larc.nasa.gov) website, including average annual earth surface skin temperature (Ts), temperature, and precipitation. Satellite images and particular latitude and longitude coordinates for the study area were provided (Fig. 1). Skin temperature (Ts) is the term used to describe the actual temperature of the earth's surface. Data on the average annual

degree of earth skin temperature from 2005 to 2022 were collected from River Kaveri, Karuri, and Tamil Nadu. For the study area, precise latitude and longitude were provided, along with satellite images (Fig. 1).

6 Human Disturbance Score

Aquatic areas' ecological and biological conditions are assessed using techniques like interviews and

Table 1 The LULC categories of Bhavani River basin, Mettupalayam, and their descriptions

Class	Description
Water body	All water bodies (lakes, rivers, streams, canals, and reservoirs)
Forest land	Including all land areas such as dense forests, open forests, and shrubs
Agricultural land	Vegetables, crops, fruits, tea plantation, and irrigated land
Built-up area	Together with all commercial, residential, and roads
Barren land	All areas of non-usable land

the human disturbance score. Water bodies are categorized into low, middle, and high impacts based on protocol method with slight modification (Gernes & Helgen, 2002). The data collected gathered various quantifiable factors to calculate the human disturbance factor. Features affecting wetlands include critical zone disturbances (0–18 points), buffer zone disturbances (0–18 points), habitat alteration (0–18 points), and hydrological alteration (0–21 points) within 50 of the wetlands' margin. QGIS yearwise maps collect data on waterbody type, hydrological conditions, land use patterns, ecological state, and habitat assessment, categorized into four categories ranging from best to poor. The human disturbance gradient score for each wetland was determined by squaring the scores from each factor. The definite range of a wetland value falls within the ranges of 0–33, 33–67, and 67–100 (Gernes & Helgen, 2002). It can be ranked as least impacted, mid-impacted, and most or highly impacted, accordingly.

7 Results

The climate data average mean and standard deviation are mentioned in Table 2. There has been a change in the earth's skin surface temperature between 1991 and 2021. We used the annual minimum of the earth's skin surface temperature, which ranged from 37.37 to 29.98 °C, with less than 28 °C including 19.35% and above being 80.65%. There is a fluctuation in their annual temperature throughout the seasons. The minimum annual temperature was 26.55 °C, and the

maximum was 28.5 °C. 19.35% contained less than 26 °C, and 80.65% contained more than 26 °C. The season varies in their annual precipitation. With a maximum of 1129 mm, the minimum yearly precipitation was 332 mm. Less than 600 mm was represented by 19.35%, 800 mm to 1000 mm by 74.19%, and 1000 mm or more by 6.45%. Human disturbance score values were categorized into three kinds. The minimum was 34 and the maximum was 75. 0–33 were least impacted (LI) was 7.40%, mid-impacted (MI) was 51.85%, and highly impacted (HI) was 40.74% in recent years.

Thirty-one years of historical data were used to analyze the earth's surface skin temperature (AM=28.53, SD=0.598) and year-to-year variations (AM=2008, SD=7.937). The correlation between earth skin temperature values is 0.152 as seen in Table 2 and Fig. 3. This suggests a marginally significant yet positive connection. The *p*-value, which is given as *p* 0.001, is 0.059 (cited under Sig. (2-tailed)), which is less than 0.05. There was no statistical significance and a positive correlation between the year and earth skin temperatures ($r=0.152$, $N=27$, $p>0.001$). The temperature fluctuates throughout the course (AM=27.42, SD=0.459). The statistic table indicates that the correlation between the temperature measurements in this instance is 0.255. This indicates a moderate positive association. The *p*-value, which is written down as *p* 0.001 and is quoted under "Sig. (2-tailed)," is 0.200, which is less than 0.05. Temperature and yearwise had a significant, positive correlation ($r=0.255$, $N=27$, $p>0.001$) and were statistically associated (Fig. 5). The yearwise changes

Table 2 The Pearson correlation coefficient variables of the study area

	Yearwise	Surface skin temperature	Annual temperature	Annual precipitation	HDS values	Mean	Std. deviation
Yearwise	1					2008.00	7.937
Surface skin temperature	0.152	1				28.53	0.598
	0.448						
Annual temperature	0.255	0.990**	1			27.42	0.459
	0.200	0.000					
Annual precipitation	0.064	-0.711**	-0.651**	1		714.68	172.483
	0.753	0.000	0.000				
HDS values	0.953**	0.251	0.343	-0.046	1	57.44	14.611
	0.000	0.206	0.080	0.821			

$N=27$, ** $p<0.1$ (2-tailed)

Fig. 3 Annual earth skin temperature

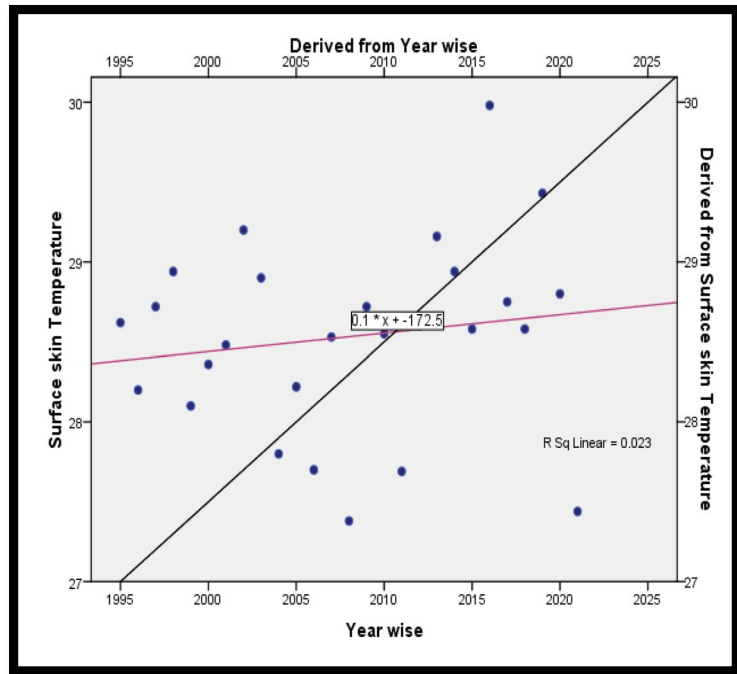


Fig. 4 Annual precipitation

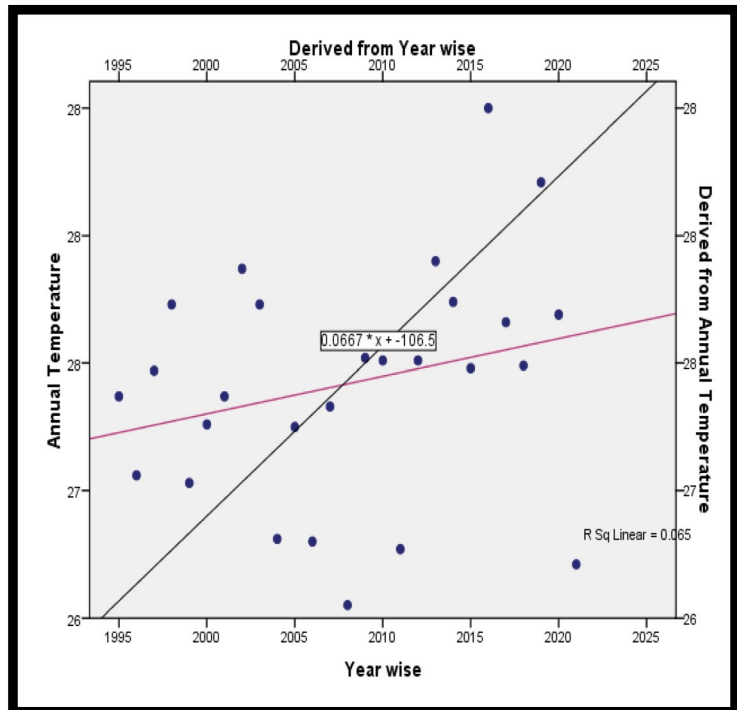
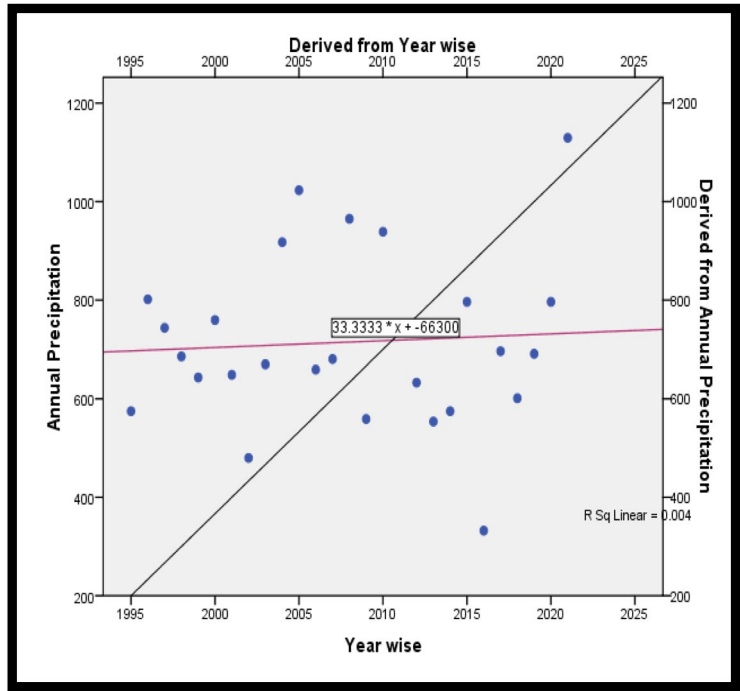


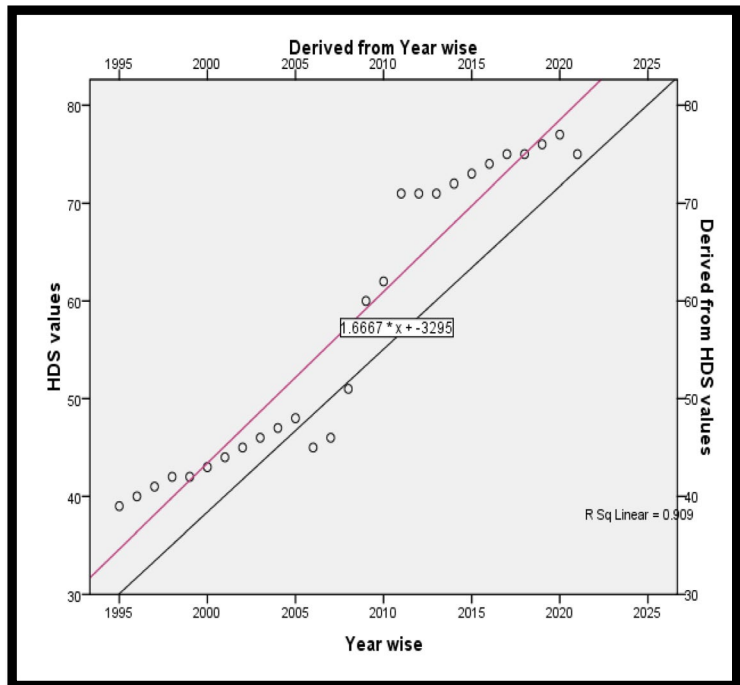
Fig. 5 Annual temperature



and precipitation were examined (AM=714.68, SD=172.483). In this instance, the correlation of precipitation value is 0.064. A non-significant

association can be shown in Fig. 4. The *p*-value, which is given as *p* 0.001, is 0.753 (cited under Sig. (2-tailed)), which is less than 0.05. The correlation

Fig. 6 HDS values



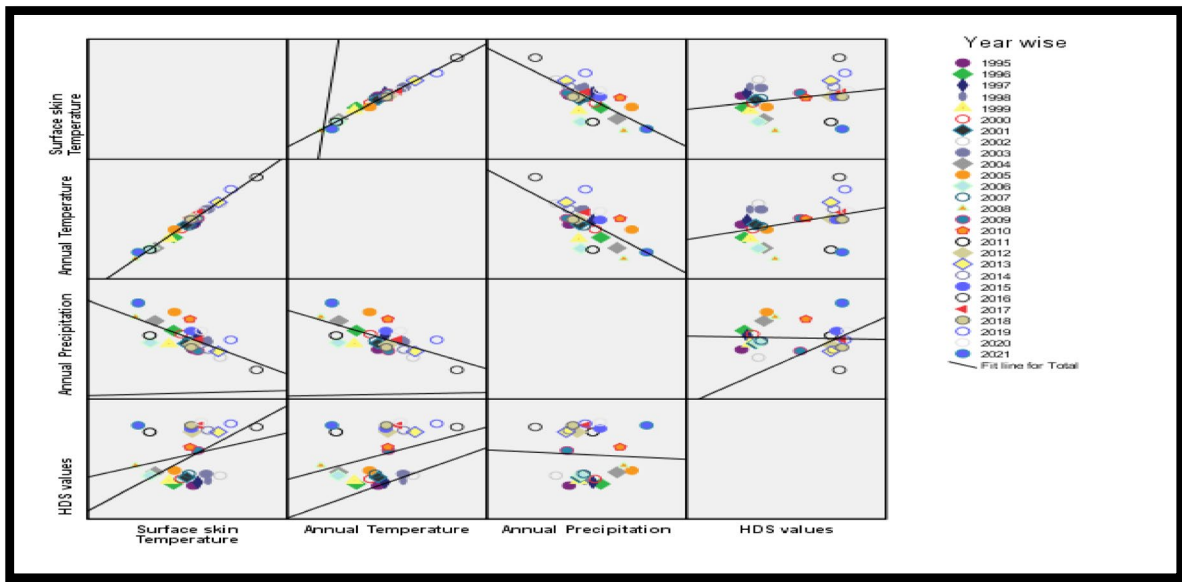


Fig. 7 Complex matrix

between the years and the precipitation was non-significant and somewhat positive ($r=0.064$, $N=27$, $p>0.001$) (Fig. 5). The correlation between the years and the HDS values was a significant positive association ($r=0.953$, $N=27$, $p>0.001$). HDS levels were associated with a substantial positive correlation ($r=0.953$, $N=27$, $p>0.001$) (Fig. 6). The HDS scores from 1995 to 1997 were least affected (LI) (0–33), then mid-impacted (MI) up to 1997–2010 (33–67), and then high impact (HI) (67–100) presently due to several human actions. The overall matrix graph is mentioned in Fig. 7.

8 Temperature Analysis

A temperature map is a type of thematic map that displays temperature data in a geographic area. Using digital elevation models, temperature maps for two different years, 2014 and 2022, have been obtained. The results show the difference between the temperatures of 2 years between the periods of 8 years, 2014 to 2022. The map shows (Figure 28) the average temperature for the year 2014 in the study area. In a blue-to-red gradient, cooler temperatures are represented by shades of blue and warmer temperatures are represented by shades of red. The map shows (Figure 19)

the average temperature for the year 2022 in the study area. From this, the change in temperature over the observed time period increased in 2022. According to data obtained from <https://weatherspark.com/h/y/108544/2011/Historical-Weather> during 2014 in Karur, India, the average temperature of Manmangalam Taluk for the year ranges from 31 to 41 °C, whereas for 2023, the temperature ranges from 32 to 40 °C, thus experiencing very low and very high temperatures comparatively. The difference in their temperature ranges can also be obtained from Figs. 8 and 9, showing changes in their raster composition.

9 Land Use and Land Cover Analysis

The land use and land cover maps shown in Figs. 10, 11, and 12 were done by the following process: the data were collected from the Landsat 8–9 OLI/TIRS for 2005, 2014, and 2022. It was further processed in QGIS. The visible bands (red, blue, and green) are composited, obtaining a multi-spectral image, and then unsupervisedly integrated, obtaining the land use and land cover image. The total area of Manmangalam is 1781 ha, where LULC was performed for the study area of 589.95 km². According to an analysis of land use and land cover classification, it was further

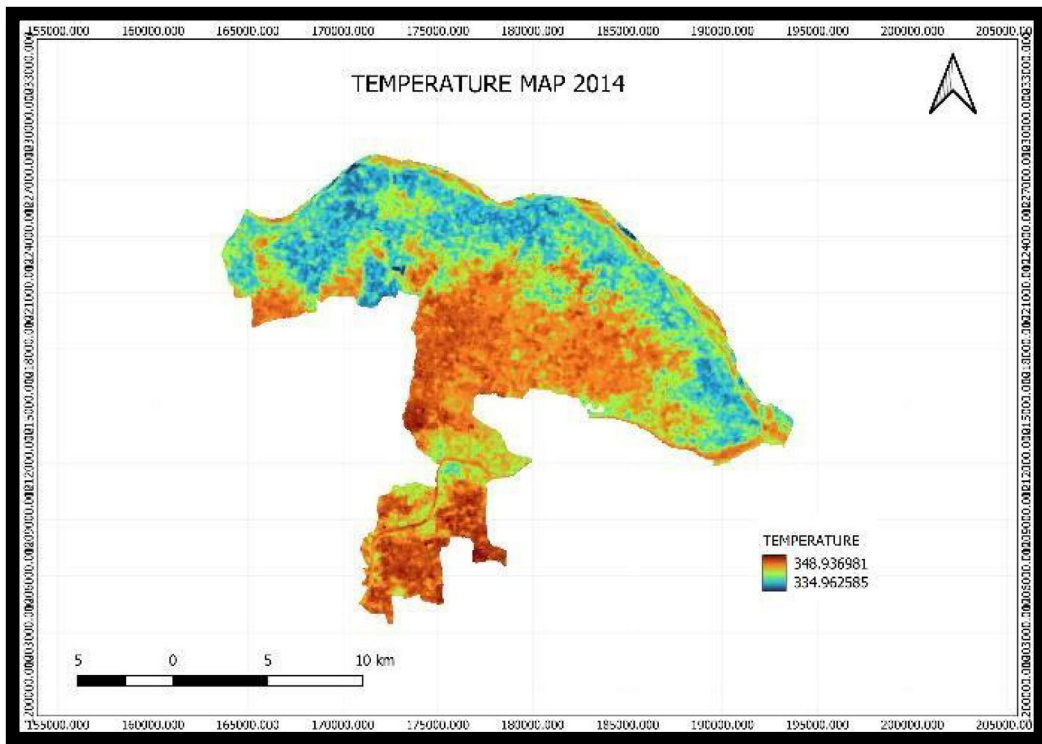


Fig. 8 Land surface temperature of Manmangalam Taluk—2014

classified into four groups: water bodies, agricultural areas, built-up areas, and barren lands. The data that has been collected from Landsat 8 has been analyzed. Generally, it refers to the categorization or classification of human activities and natural elements on the landscape within a specific time frame. The majority of the area has been covered by the built-up area. The overall LULC map is mentioned in Figure 10 and Fig. 13 for 2005; the LULC map for 2014 is mentioned in Figure 11 and Fig. 14; and the LULC map for 2022 is mentioned in Figure 12 and Fig. 15. The individual classifications of the LULC map in the year 2005 are mentioned in Figure 17 for water bodies, Figure 20 for agricultural land, Figure 23 for built-up areas, and Figure 24 for barren land. The individual classifications of the LULC map in the year 2014 are mentioned in Figure 18 for water bodies, Figure 21 for agricultural land, Figure 24 for built-up areas, and Figure 27 for barren land.

According to the analysis of LULC, we further classified into five groups such as forest, water bodies, agrarian land, built-up, and barren lands. From

the data that have been collected from Landsat 5 and Landsat 8, the heterogeneity of land cover has been analyzed. LULC is a generic term for the classification of human actions and usual phenomena on the landscape inside a specific time scale. The overall LULC map is mentioned in Figure 10 and Fig. 7 for the year 2004, Figure 11 and Fig. 14 for the year 2014, and Figure 12 and Fig. 15 for the year 2022. The individual classification of the LULC map in the year 2022 is mentioned in Figure 19 for water bodies, Figure 22 for agricultural land, Figure 25 for built areas, and Figure 28 for barren land.

The outcomes of LULC categorization for the Landsat 5 image show that all courses receive the same amount of LULC. Agricultural areas cover about 177.01 km² (30.01%) of the total study zone. The next major area includes built-up land of 172.17 km² (29.18%), barren land area of 131.81 km² (22.34%), and water bodies of 108.97 km² (18.47%).

The classification report for the year 2005 is mentioned in Table 3 representing both the area and their percentage. The total error matrix for the

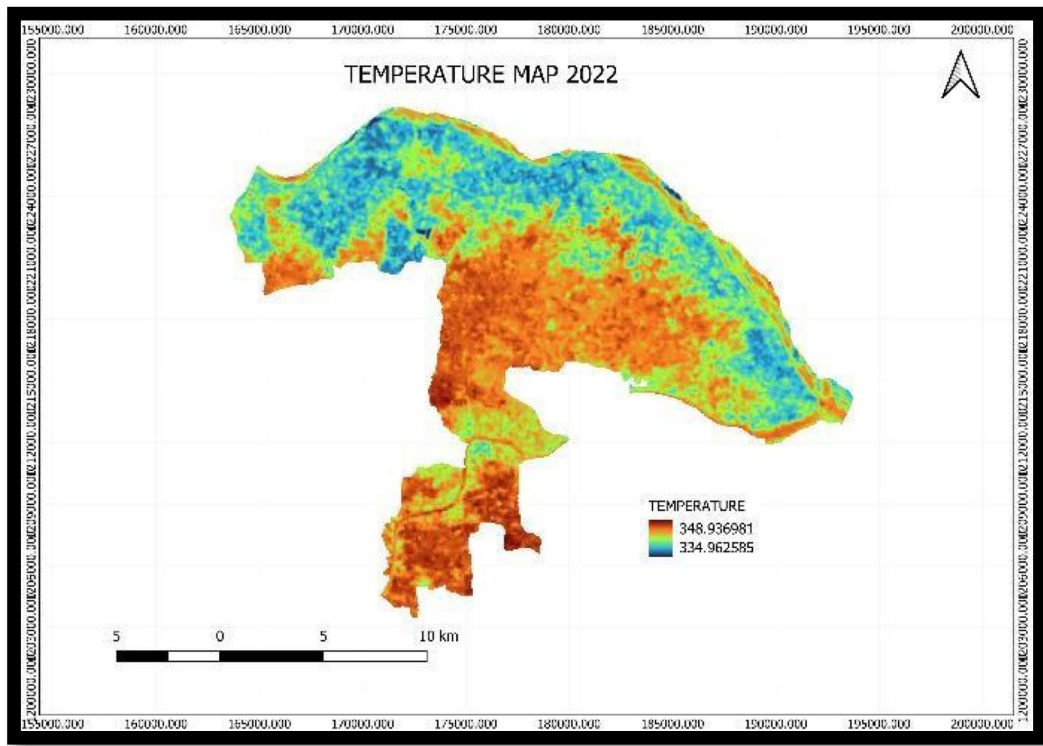


Fig. 9 Land surface temperature of Manmangalam Taluk—2022

year 2005 is mentioned in Table 4. The total error matrix for waterbodies was 121,080; agricultural areas 196,682; built-up lands 191,311; and barren land 146,448. The change matrix (Fig. 16) is mentioned above. The area units were recorded in square kilometers (km^2); standard error (SE), confidence interval (CI), producer's accuracy (PA), kappa efficiency, and user's accuracy (UA) were also observed for our study. The overall accuracy is 100.00%, the kappa efficiency of 1.00 was observed in our study, and the data are mentioned in Table 5.

The LULC assessment outcomes for the Landsat 5 image for the year are determined according to the data from 2014; the majority of LULC in every level goes to the agricultural areas, which cover about 209.94 km^2 (35.58%) of the full study area. The next major area includes agricultural lands covering 167.14 km^2 (28.33%). The barren land covers an area of 142.79 km^2 (24.29%). Water bodies cover an area of 70.08 km^2 (11.87%) which majorly includes the river basins. The individual

classifications of the LULC map in the year 2005 are mentioned in Figure 17 for water bodies, Figure 21 for agricultural land, Figure 23 for built-up areas, and Figure 26 for barren land.

The classification report for the year 2014 is mentioned in Table 5 representing both the area and fraction of kinds of land cover that exist in the studied site. The total error matrix for the year 2014 is mentioned in Table 5. The total error matrix for waterbodies was 77868, agricultural areas 185,713, built-up lands 158,665, and barren land 233,274. The change matrix is mentioned in Figs. 13 and 14. The individual classifications of the LULC map in the year 2014 are mentioned in Figure 18 for water bodies, Figure 21 for agricultural land, Figure 24 for built-up areas, and Figure 27 for barren land.

The results of LULC classification for the Landsat 8–9 OLI/TIRS 2022 image show that the greatest share of LULC from all classes goes to the built-up areas, as an increase in settlement built-up covers an area of 250.70 km^2 (42.49%), which is a tremendous

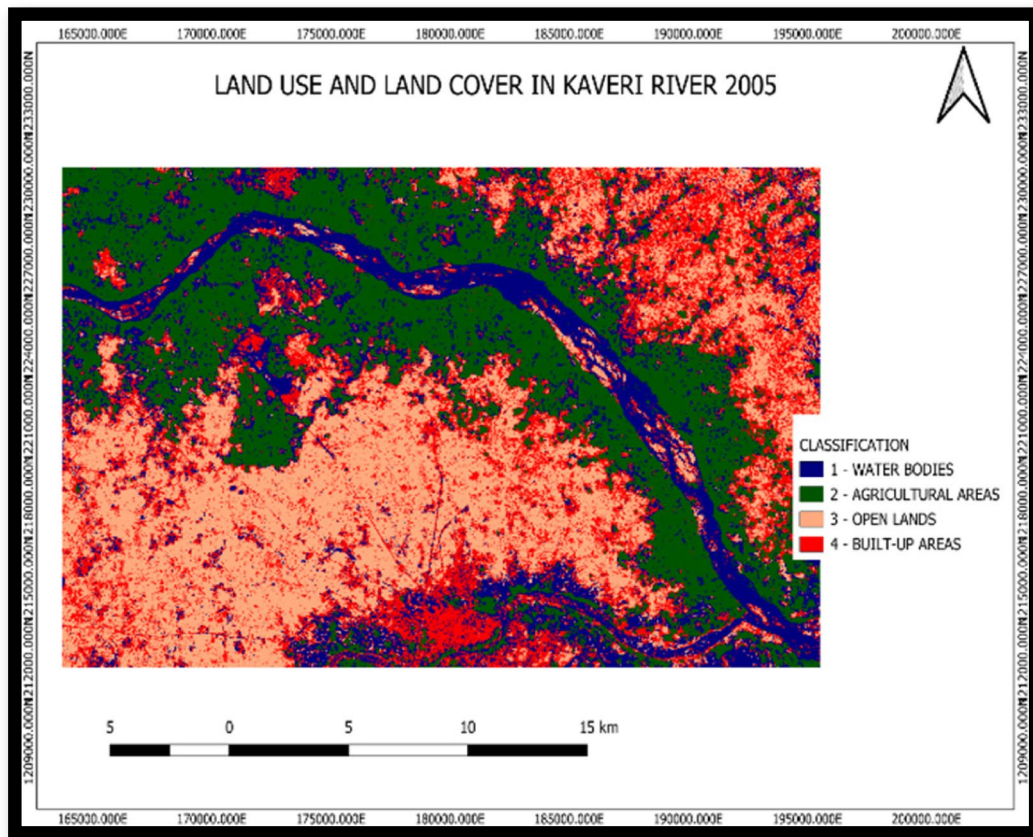


Fig. 10 LULC of Kaveri River—2005

increase compared with the previous data of 2014. The next major area includes open lands covering an area of 168.93 km² (28.63%). The agricultural area covers an area of 148.67 km² (25.20%), which mostly includes the river basins. The least area is being covered by the water bodies, which are about 21.64 km² (3.66%) and mostly include the river basin. However, the comparative study shows that in the past 8 years, there has been a tremendous increase in settlements by the human population, which has greatly increased urbanization and reduced the natural land area (Table 6).

The total error matrix for the year 2023 is mentioned in Table 7. The total error matrix for water bodies was 24039, agricultural areas 164,816, built-up lands 187,601, and barren land 278,458, which were observed (Table 10).

The overall accuracy is 100.00% and the kappa efficiency is 1.00, which was observed in our study. The unit measure is mentioned in Table 8.

For LULC, we have classified four classes: water-bodies, agricultural areas, built-up land, and barren land. We also selected two different periods, 2005 and 2014, for change detection. Fig. 6 shows the results, like the built-up area being the dominant class in our study area. The results of LULC classification for the Landsat 5 thematic mapper (TM) image show that the greatest share of LULC from all classes goes to the built-up areas, which cover about 172.01 km² (29.18%) of the total study area. The next major area includes agricultural lands covering an area of 177.01 km² (30.01%). Water bodies cover an area of 108.97 km² (18.47%), which mostly includes the river basins. The barren areas cover an area of about 131.84 km² (22.34%) (Tables 9, 10).

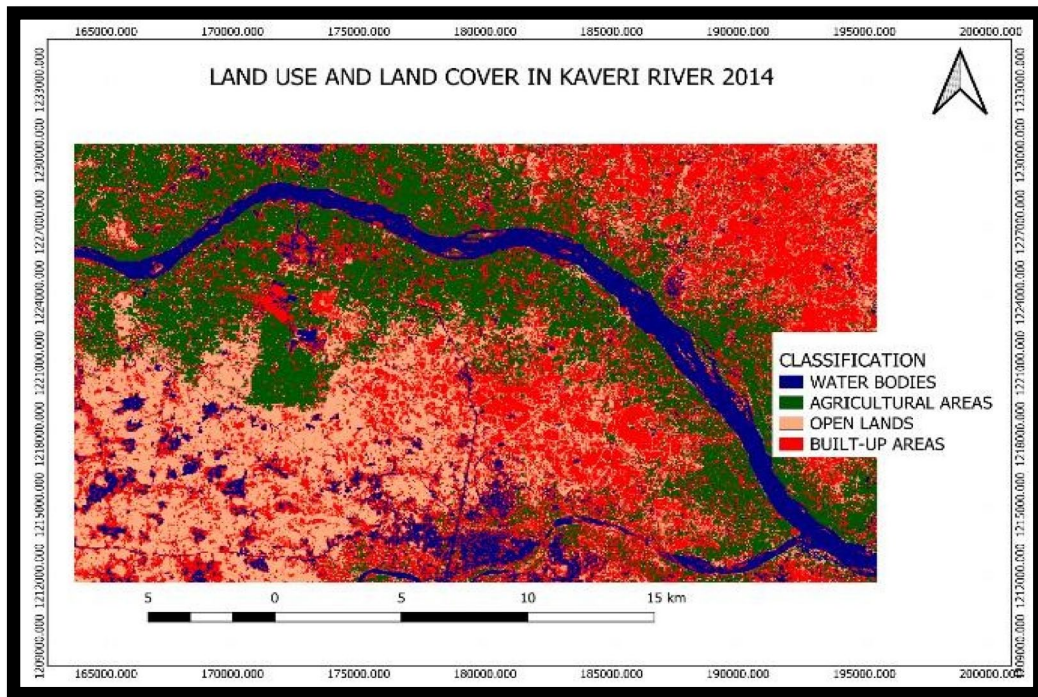


Fig. 11 LULC of Kaveri River—2014

For LULC, we have classified four classes: water-bodies, agricultural areas, built-up land, and barren land. We also selected two different periods, like 2014 and 2022, for change detection. Fig. 16 shows the results, like the built-up area being the dominant class in our study area. The results of LULC classification for the Landsat 5 thematic mapper (TM) image show that the greatest share of LULC from all classes goes to the built-up areas, which cover about 209.94 km² (35.58%) of the total study area. The next major area includes agricultural lands covering an area of 167.14 km² (28.33%). Water bodies cover an area of 70.08 km² (11.87%), which mostly includes the river basins. The barren areas cover an area of about 142.79 km² (24.20%). The individual classifications of the LULC map in the year 2023 are mentioned in Figure 19 for water bodies, Figure 22 for agricultural land, Figure 25 for built-up areas, and Figure 28 for barren land.

10 Land Use Changes

The results of LULC classification for the Landsat 8–9 OLI/TIRS 2014 image show that the greatest

share of LULC from all classes goes to the built-up areas, which cover about 209.94 km² (35.58%) of the total study area. The next major area includes agricultural lands covering an area of 167.14 km² (28.33%). Water bodies cover an area of 70.08 km² (1.857%), which mostly includes the river basins. The barren areas cover an area of about 6.850 km² (5.525%). The results of LULC classification for the Landsat 8–9 OLI/TIRS 2022 image show that the greatest share of LULC from all classes goes to the built-up areas, which cover about 209.94 km² (35.58%) of the total study area. The next major area includes agricultural lands covering an area of 167.14 km² (28.33%). Water bodies cover an area of 70.08 km² (1.857%), which mostly includes the river basins. The barren areas cover an area of about 6.850 km² (5.525%). Accuracy evaluation is an important stage in evaluating an individual's performance in regard to how effectively the classification was accomplished, as well as a tool for analyzing the use of a categorized image. It is a useful measuring parameter in change detection (CD). Landsat pictures are categorized into different land cover classes and then compared to reference data. The visual analysis of initial Landsat visuals,

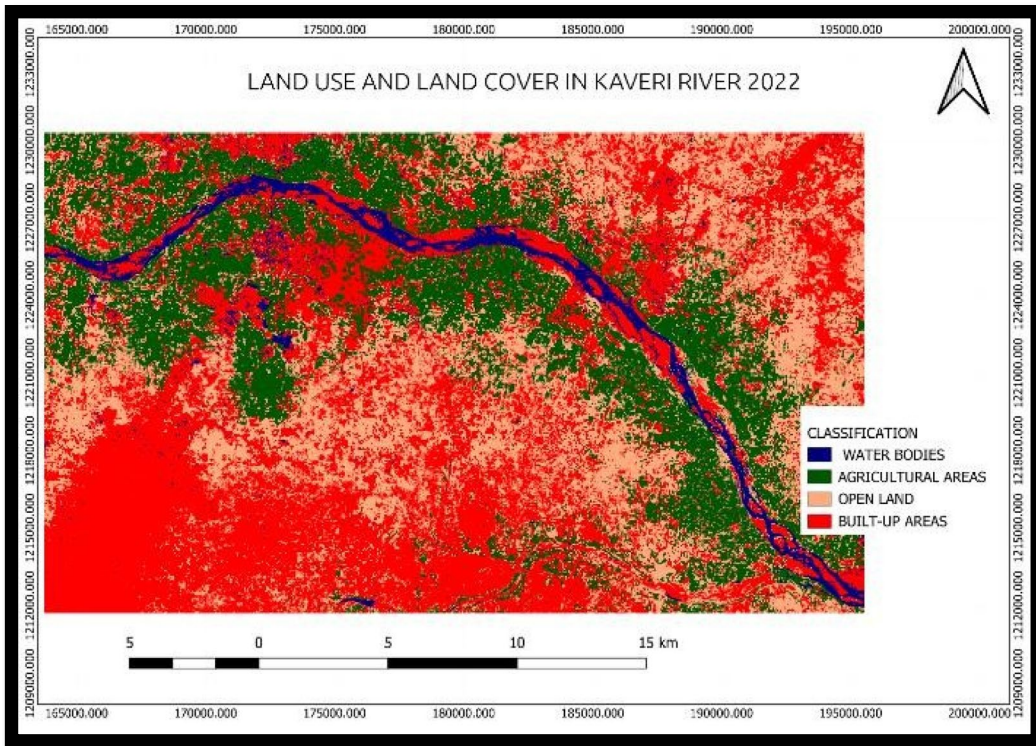


Fig. 12 LULC of Kaveri River—2022

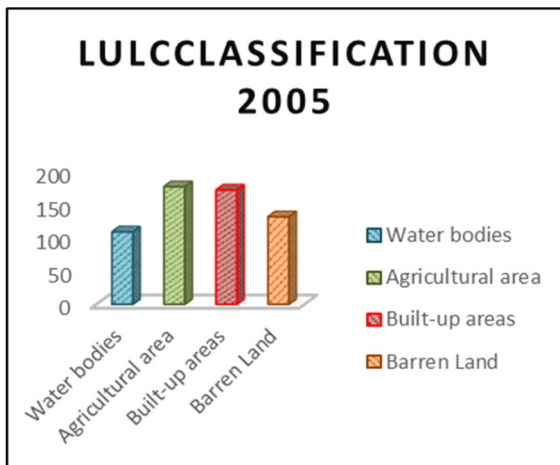


Fig. 13 LULC of Kaveri River in 2005

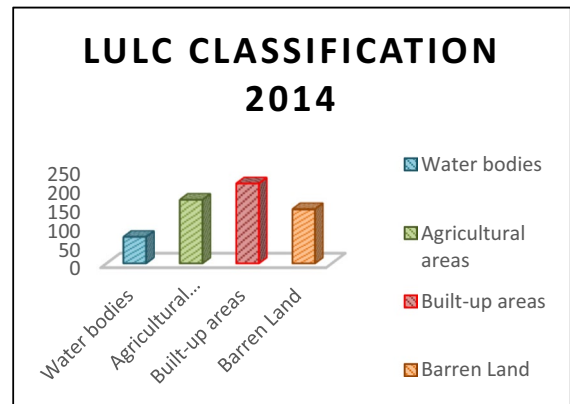


Fig. 14 LULC of Kaveri River in 2014

photos from earth on Google at a high resolution, and a physical examination of the research area were used to provide reference data for each categorized LULC class. The classified image and actual data are nearly

the same if the kappa coefficient is greater than 0.81. The overall accuracy of our categorized images, as well as the associated kappa coefficient of 85–90% for LULC visualization, demonstrates that there is virtually full agreement between the classified picture and

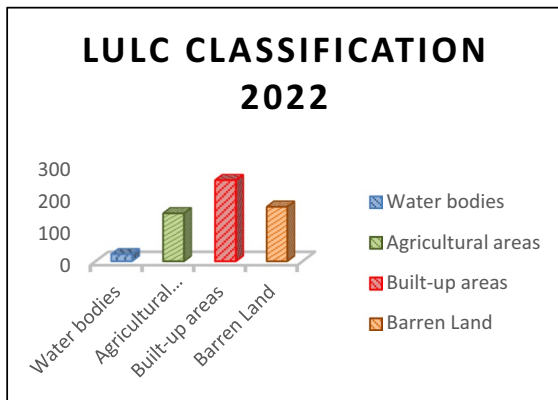


Fig. 15 LULC of Kaveri River in 2022

the source image, indicating that the LULC mapping is better categorized. Finally, the post-classification change identification technique is applied by comparing classed photos, creating final LU/LC maps, and analyzing the LULC trends along with its primary moving elements in the study area.

Figures 17, 18, 19, 20, 21, 22, 23, 24, 25, 26, 27, and 28 represent the variations in the individual land uses of the study area in Manmangalam Taluk in the Karur District.

Average seasonal rainfall (mm) received in the study area from 2001 to 2022.

11 Discussion

In climate research, scale is crucial. The characteristics or even the indications may vary from a single scale to the next. To acquire an entire perspective of an issue, one must investigate it at many spatial or temporal scales. The causes for the Tskin and Tair variations vary in our research as well, which was influenced by cloud cover, and the worldwide spread of Tskin fluctuates with area heat based on the sunlight zenith direction. The amount of surface heat returns towards outer space influences skin temperature. The worldwide, year-averaged skin temperature follows the same pattern as surface albedo, being hot in July while cold in January and December. In our investigation, we found that yearly, the earth's skin surface temperature increased from 23.33 to 25.99 °C between 1991 and 2001. Their average temperature varies during each year. The earth's surface skin temperature and year-to-year changes were studied using 31 years of historical data. There was no statistical significance but a positive link between the year and the temperature of the earth's skin temperature was

Table 3 LULC classification and matrix table report for the year 2005

Class	Water bodies	Agricultural areas	Built-up areas	Barren lands	Total	Pixel sum	Percentage, %	Area, km ²
Water bodies	121,080				121,080	121,080	18.47	108.97
Agricultural areas		196,682			196,682	196,682	30.01	177.01
Built-up areas			191,311		191,311	191,311	29.18	172.17
Barren lands				146,448	146,448	146,448	22.34	131.81
Total	121,080	196,682	191,311	146,448	655,521			

Table 4 Area-based error matrix represented in 2005

Class	Water bodies	Agricultural areas	Built-up areas	Barren lands	km ²
Water bodies	0.18				108.97
Agricultural areas		0.3			177.01
Built-up areas			0.29		172.17
Barren lands				0.22	131.81
Total	0.18	0.3	0.29	0.22	589.96
Area	108.97	177.01	172.17	131.8	589.96

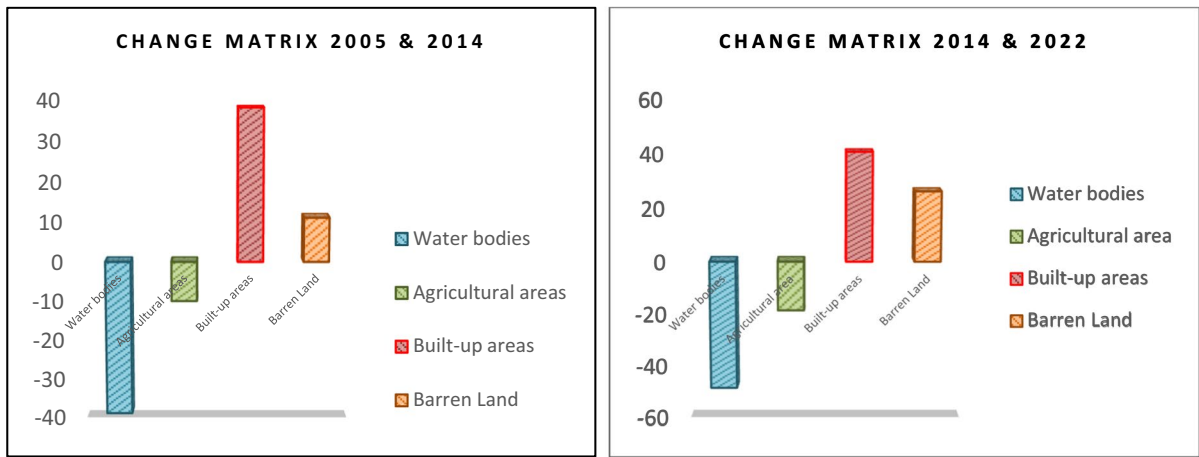


Fig. 16 Change matrices of LULC classes between 2005–2014 and 2014–2022 in Bhavani River

Table 5 LULC classification and matrix table report for the year 2014

Class	Water bodies	Agricultural areas	Open lands	Built-up areas	Total	Pixel sum	Percentage, %	Area, km ²
Water bodies	77,868				77,868	77,868	11.87	70.08
Agricultural areas		185,713			185,713	185,713	28.33	167.14
Open lands			158,665		158,665	158,665	24.2	142.79
Built-up areas				233,274	233,274	233,274	35.58	209.94
Total	77,868	185,713	158,665	233,274	655,521			

Table 6 Area-based error matrix represented in 2014

Class	Water bodies	Agricultural areas	Open lands	Built-up areas	Area (km ²)
Water bodies	0.11				70.08
Agricultural areas		0.28			167.14
Open lands			0.24		142.79
Built-up areas				0.35	209.94
Total	0.11	0.28	0.24	0.35	589.96

Table 7 LULC classification and matrix table report for the year 2022

Class	Water bodies	Agricultural areas	Open lands	Built-up areas	Total	Pixel sum	Percentage, %	Area, km ²
Water bodies	24,039				24,039	24,045	3.66	21.64
Agricultural areas		164,816			164,816	165,197	25.2	148.67
Open lands			187,601		187,601	187,704	28.63	168.93
Built-up areas				278,458	278,458	278,563	42.49	250.7
Total	24,039	164,816	187,601	278,458	655,521			

Table 8 LULC area-based error matrix in 2022

Class	Water bodies	Agricultural areas	Open lands	Built-up areas	Area (km ²)
Water bodies	0.03				21.63
Agricultural areas		0.25			148.33
Open lands			0.28		168.84
Built-up areas				0.42	250.61
Total	0.03	0.25	0.28	0.42	589.96

Table 9 Change matrix of LULC between the years 2005 and 2014

Land use type		2005	2014	Change matrix
Water bodies	Area (km ²)	108.97	70.08	38.89
	%	18.47	11.87	6.6
Agricultural area	Area (km ²)	177.01	167.14	9.87
	%	30.01	28.33	1.68
Built-up areas	Area (km ²)	172.01	209.94	-37.93
	%	29.18	35.58	-6.4
Barren land	Area (km ²)	131.81	142.79	-10.98
	%	22.34	24.2	-1.86

Table 10 Change matrix of land use types for 2014 and 2022

Land use type		2014	2022	Change matrix
Water bodies	Area (km ²)	70.08	21.64	48.44
	%	11.87	3.66	8.21
Agricultural area	Area (km ²)	167.14	148.67	18.47
	%	28.33	25.2	3.13
Built-up areas	Area (km ²)	209.94	250.7	-40.76
	%	35.58	42.49	-6.17
Barren land	Area (km ²)	142.79	168.93	-26.14
	%	24.2	28.63	-4.43

observed. Temperature maps, which are thematic maps that display temperature data in a geographic area, are often used to visualize and analyze temperature changes over time. Using digital elevation models, temperature maps for two different years, 2014 and 2022, have been obtained for the study area. The results show the difference between the temperatures of the 2 years over the period of 8 years, from 2014 to 2022. In 2014 in Karur, the average temperature for the year ranged from 31 to 41 °C. However, for

2023, the temperature ranges from 32 to 40 °C, indicating a slight decrease in the temperature range. The key physical factor influencing water's temperature (Gresselin et al., 2021) and in general (Caissie, 2006) is shifts in the seasons. Our research also found that temperature fluctuations occurred through both the summer and winter seasons from February to May. The temperature and yearwise data had a statistically significant, positive association. According to Bal et al. (2016), the whole state of Tamil Nadu projection showed that the end of the century indicates warmer summer, with maximum temperature increasing by about 3.1 °C.

The rise in severe rainfall and the predicted reduction in total rainfall in dry places (Marvel & Bonfils, 2013; Tabari & Willems, 2018) reinforce the "it rarely rains, but it showers" pattern (Trenberth, 2015). The shifts in their yearly rainfall were additionally confirmed in our investigation. During the time of the monsoons from June to August, a maximum of 1383 mm was recorded, with an average of 450 to 1380 mm recorded. The link between the years and precipitation was considerable, as evidenced by the positive association displayed above. Modest flows are expected to decrease with global warming across a much greater area than average yearly runoff drops (Döll & Schmied, 2012), whereas high drifts are expected to raise extra than average annual drainage (Arnell & Gosling, 2013). According to our research, the rainy season has increased rain, notably from June to September. Also, it stated that there is a slight decrease in rainfall during the northeast monsoon season (October–December) (Krishna Kumar et al., 2011). The estimate for the last decade of the decade implies a small drop in rainfall during monsoons across all of Tamil Nadu. Human activities have an opportunity to increase stressors to river operative (Tickner et al., 2020; Vörösmarty et al., 2010). However, in recent years, the changes have been more pronounced

Fig. 17 LULC representing water bodies—2005

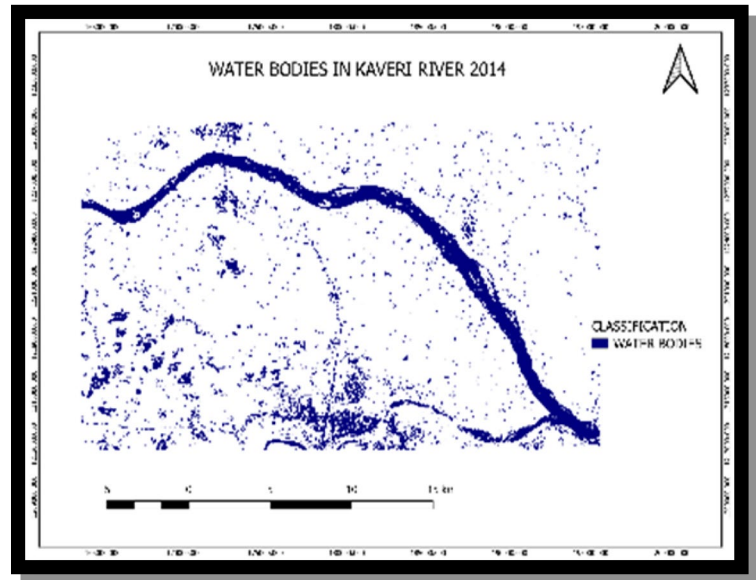
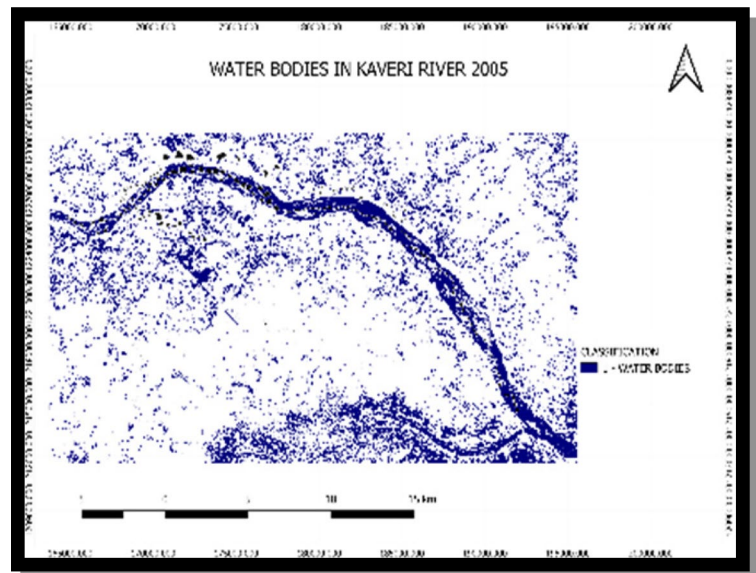


Fig. 18 LULC representing water bodies—2014



due to an increase in settlements and changing agricultural practices, which impact hydrological processes by altering interception, eva-transpiration, and infiltration rates, thus affecting water resources. The water flow in rivers, lakes, and reservoirs differs critically seasonally and year to year. The buffer bands' preservation is a significant aspect of determining their long-term nutritional value.

According to the strong correlation between past years' data on the HDS scores, river change is

triggered by a variety of variables. In our research area, hydrological change induced by size contraction, location, and dryness is an important cause of aquatic decline in ecosystems. River basins, which are essential components of the natural creation of water resources, are facing an irreversible water crisis (Zhang et al., 2018). Human activities can exacerbate the shortage of water and alter flow patterns at the local (Laizé et al., 2014) and world (Veldkamp et al., 2018) scales, according to evidence. In our study,

Fig. 19 LULC representing water bodies—2022

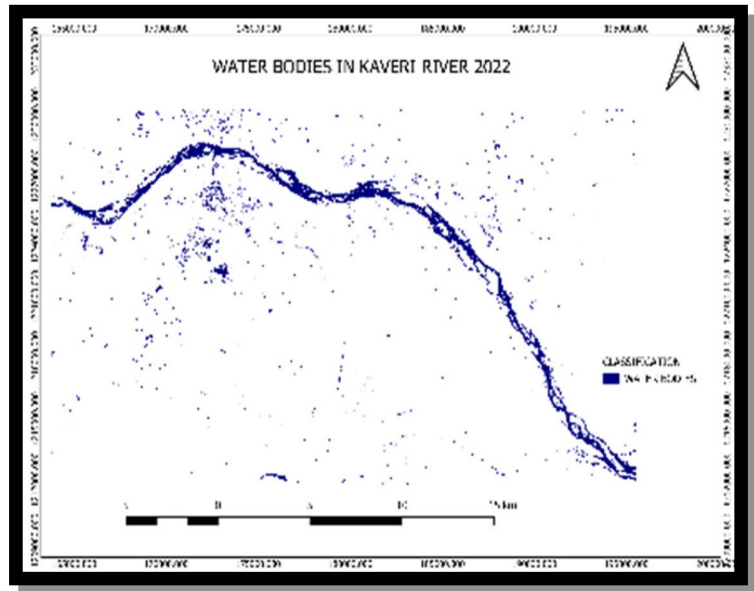
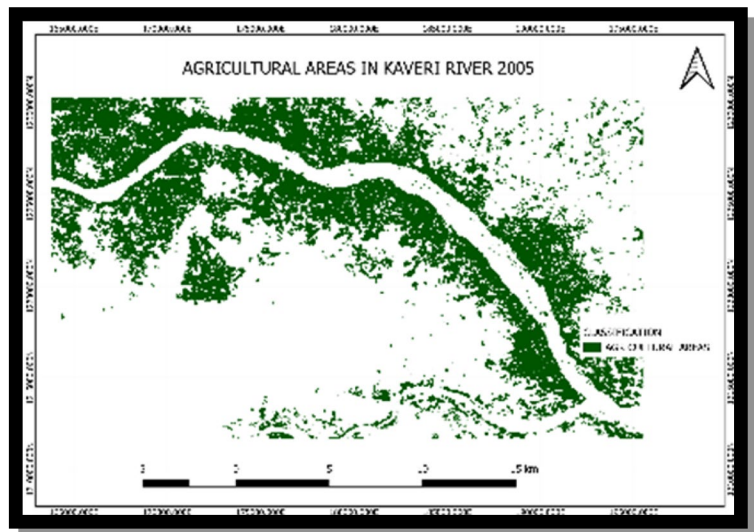


Fig. 20 LULC representing agricultural areas—2005



HDS scores 0–33 were classified as least influenced (LI) at 70.96%, mid-impacted (MI) at 22.58%, and highly impacted (HI) at 6.45% in the last few years due to many anthropogenic activities. Because of several anthropogenic activities, the correlation between the years and the HDS values showed a substantial positive association. Also, our research found that greater HDS levels are triggered by human activities. The LULC map provides information on the spreading of diverse kinds of LULC in a particular area. It is a central device for environmental monitoring, natural

source management, urban planning, and disaster management. In this case, the LULC map was generated using Landsat satellite imagery for the years 2014 and 2022, covering an area of 589.95 km² in the Manmangalam Taluk. The satellite imagery was processed using QGIS software to generate a composite of visible bands (red, green, and blue), which was then classified into four major land use/land cover types: water bodies, agricultural areas, built-up areas, and barren lands. The results of the LULC classification for 2014 and 2022 were compared to analyze the

Fig. 21 LULC representing agricultural areas—2014

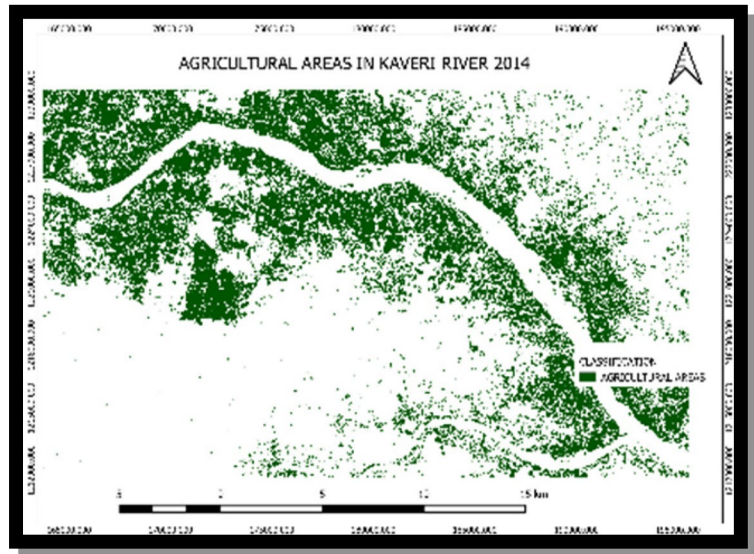
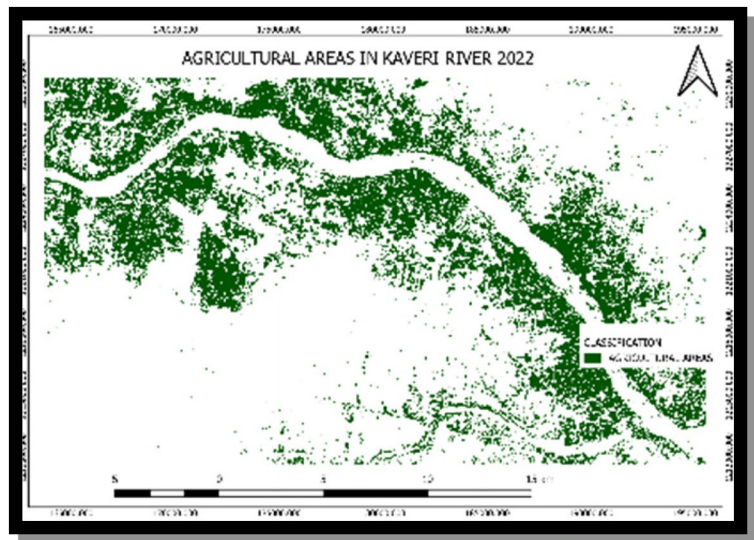


Fig. 22 LULC representing agricultural areas—2022



changes that occurred over time. The change matrix shows the zone enclosed by respective land use type in 2014 and 2022, as well as the change that occurred in each category over the 8 years. Between 1991 and 2020, the built-up area rose dramatically. It has more than doubled in size. It was 17% in 1991 and is expected to reach 40% by 2020. This could be owing to a rise in the textile sector, bus manufacturing, and related businesses. In addition to this, the neighborhood houses multiple government departments such as the Collectorate, the Court, and the SP office, as well as many private organizations. As a result of

this, the number of organizations and roadways has grown (Ravichandran & Manonmani, 2021). In our study, the analysis revealed that built-up areas are the dominant land use type in the study area, covering 209.94 km² (35.58%) in 2014 and 250.70 km² (42.49%) in 2022. Water bodies covered an area of 70.08 km² (11.87%) in 2014 and 21.64 km² (3.66%) in 2022 due to less water holding capacity and blocking water channels. This shows that Karur town is a fast-growing barren terrain, which is also being developed for additional uses such as settlement, industry, and transportation. In 1991, 58% of barren land was

Fig. 23 LULC representing built-up areas—2005

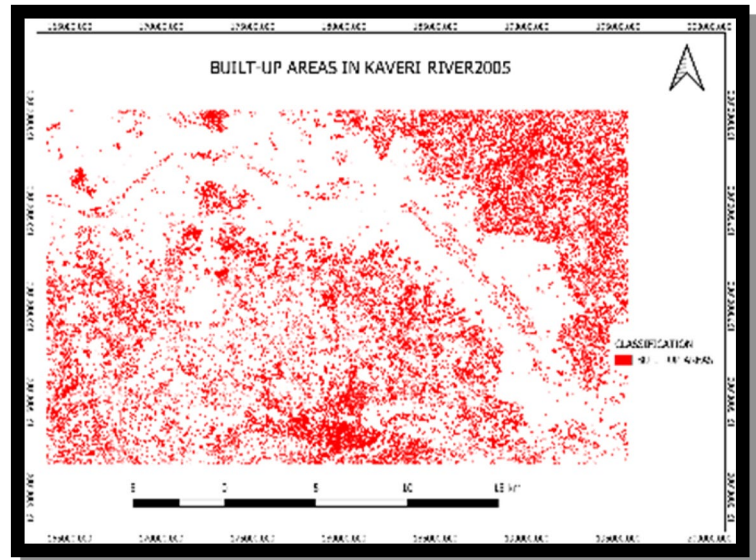
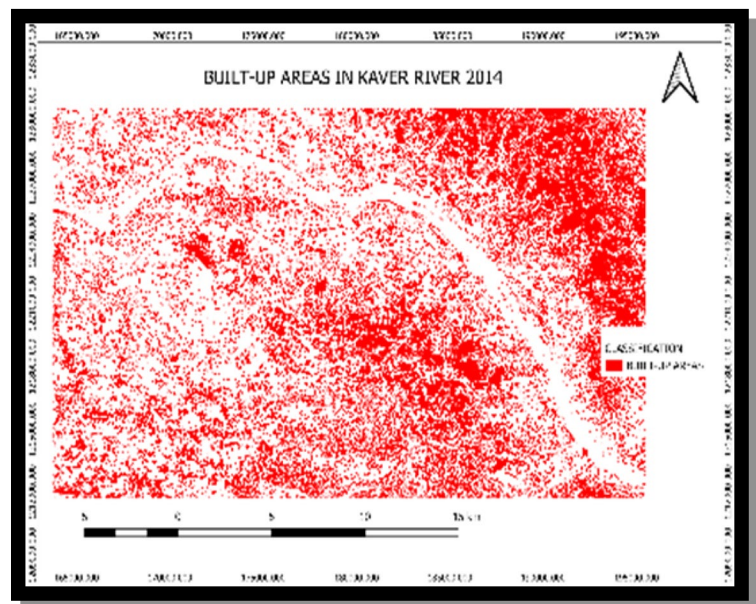


Fig. 24 LULC representing built-up areas—2014



barren, which decreased to 53% in 2000. Barren land declined by 18% during the last four decades, from 1991 to 202 (Ravichandran & Manonmani, 2021). Urbanization due to the rapid increase in population causes severe problems with land use and land cover changes in the river basin. This demonstrates that Karur town has grown increasingly populated. In recent decades, the Karur town has expanded in the south and along the highways. The building of a flyover route from Trichi to Namakkal and from Dindigul

to Namakkal or Salem is progressing quickly (Ravichandran & Manonmani, 2021). It is construed that there is uncertainty in cultivation in this study area due to globalization. The majority of the cultivators have left their profession and engaged themselves in some other profession. Due to that, the cultivatable land has been left as barren lands (Suvetha & Maniyosai, 2018). In our study, barren lands covered 142.79 km² (24.20%) in 2014 and 168.93 km² (28.63%) in 2022.

Fig. 25 LULC representing built-up areas—2022

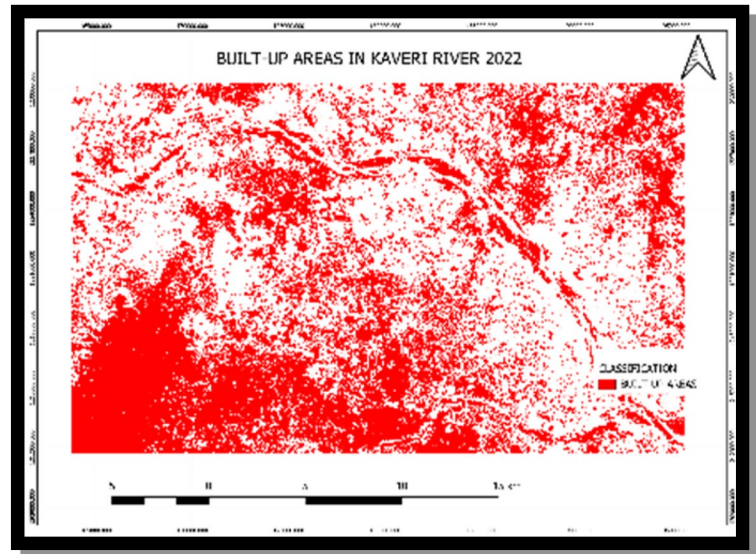
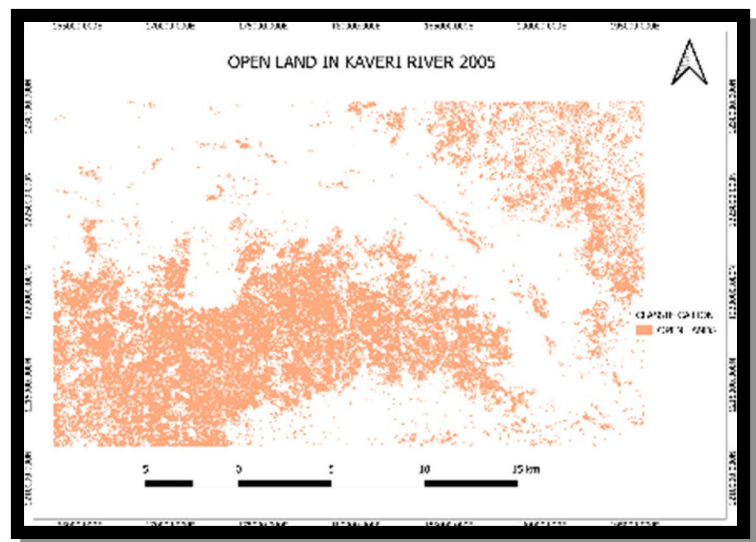


Fig. 26 LULC representing barren areas—2005



Overall, the LULC map and associated analysis provide valuable data on the distribution of LULC in the Manmangalam Taluk over time. Future climate change in the whole of Tamilnadu shows that a reduction in yield is expected due to increases in temperature and changes in rainfall (Geethalakshmi & Dheebakaran, 2008). The proportion of cultivated land was 25% in 1991 and decreased by 1% in 2000. Between 2010 and 2020, a significant amount of farmland was turned into non-agriculture property. In a decade (2010 to 2020), over 14% of good agricultural land was converted. In our study, agricultural areas

are the second-largest land use type, covering 167.14 km² (28.33%) in 2014 and 148.67 km² (25.20%) in 2022. The preference for comfortable residential areas has begun to rise in recent years mentioned by many researchers (Tagıl & Ersayın, 2015; Ozturk et al., 2021; Cetin & Sevik, 2016; Bozdogan et al., 2019; Işınkaralar & Varol, 2021; Isınkaralar & Ramazan, 2021; Cetin, 2015, 2017; Ozturk & Isınkaralar, 2019). According to Iyappan and Maria (2014), in the Namakkal district, LULC changes are noteworthy. They were triggered by increased population density and subsequent socioeconomic activities such as

Fig. 27 LULC representing barren areas—2014

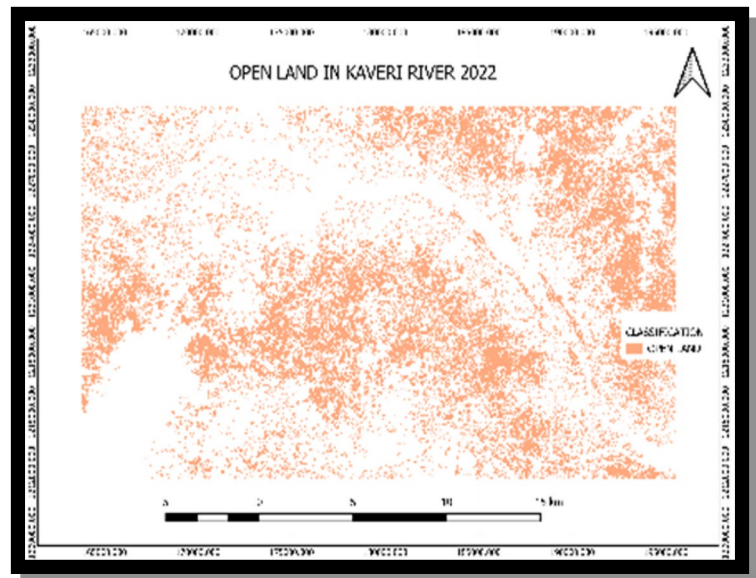
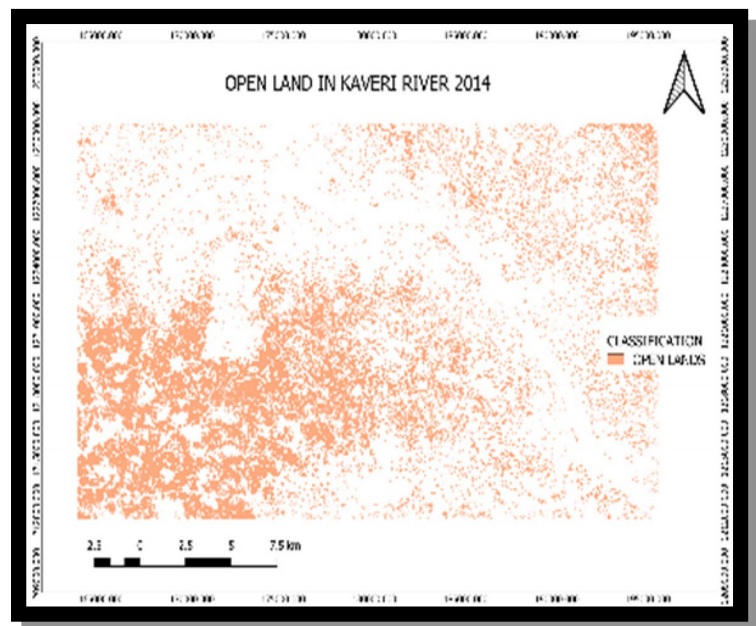


Fig. 28 LULC representing barren areas—2022



uncontrolled immigration, charcoal business, shifting cultivation, opening up of improved highways, and pastoralism.

12 Conclusion

This is the first climate impact report across the entire Kaveri river basin. Global warming is anticipated to

significantly alter ecologically critical flow phases in the Kaveri River basin, creating additional potent anxiety for river ecosystems in addition to existing anthropogenic stressors. Rivers and the ecological services they provide are increasingly under threat as a result of land use changes, population development, pollutant discharges, dam and divert flow-regime shifts, and too much groundwater extraction. Climate change can exacerbate and multiply these

dangers by altering rainfall, temperature, and runoff patterns, as well as altering biological populations and breaking ecological links in any given location. Climate adaptation strategies and mitigation measures that anticipate longer and drier times with low flows, in especially, could aid in averting major damage to river ecosystems in the future. Thus, monitoring the LULC change is considered a vital piece for assessing and determining landscape changes or environmental vigor. Costing at dissimilar spatiotemporal scales helps to assess the parameters better. Appraisal of the LULC change matrix is highly important in evaluating the status of each land cover at two different times, which is useful for determining environmental health and ecosystem administration, species saving, land use setting up, and source executive which results in largely sustainable ecological running. The hydrological situation in the watershed is expected to deteriorate (become significantly divergent) in future years at the sampling places, necessitating additional investigation. The distribution of land use and land cover in the Manmangalam Taluk shows that built-up areas are the dominant land use type in the area, covering 35.58% of the land in 2014 and 42.49% in 2022. The temperature maps for 2014 and 2022 show a slight decrease in temperature range over 8 years. This suggested GIS practice is apt for the investigative region, Bhavani River, Mettupalayam. These results can be effectively used for hydrological modeling, land use planning, watershed studies, reservoir operation, and reservoir planning.

Acknowledgements I owe sincere thanks to the management, secretary, and principal of PSG College of Arts and Science (Autonomous), Coimbatore, for providing all the facilities in the college to do the project work.

Author Contribution Jeevitha Palanisamy^b: investigation, data collection, formal analysis, visualization, writing—original draft. Dr. Varunprasath Krishnaraj^{a*}: supervision, conceptualization, final analysis, writing review, and editing. All authors read and approved the final manuscript.

Data Availability Data will be made available on request.

Declarations

Competing Interests The authors declare no competing interests.

References

- Abass, K., Adanu, S. K., & Agyemang, S. (2018). Peri-urbanisation and loss of arable land in Kumasi Metropolis in three decades: Evidence from remote sensing image analysis. *Land Use Policy*, 72, 470–479. <https://doi.org/10.1016/j.landusepol.2018.01.013>. Accessed 13 Jan 2018
- Abrantes, P., Fontes, I., Gomes, E., & Rocha, J. (2016). Compliance of land cover changes with municipal land use planning: Evidence from the Lisbon metropolitan region (1990–2007). *Land Use Policy*, 51, 120–134. <https://doi.org/10.1016/j.landusepol.2015.10.023>
- Aduah, M. S., & Baffoe, P. E. (2013). Remote sensing for mapping land-use/ cover changes and urban sprawl in Sekondi-Takoradi, Western region of Ghana. *The International Journal of Engineering and Science (IJES)*, 2(10), 66–72. <https://doi.org/10.6084/M9.FIGSHARE.848547.V1>
- Adiguzel, F., Cetin, M., Kaya, E., Simsek, M., Gungor, S., & Bozdogan Sert, E. (2020). Defining suitable areas for bioclimatic comfort for landscape planning and landscape management in Hatay Turkey. *Theoretical and Applied Climatology*, 139(3), 1493–1503.
- Ahn, J. M., Kwon, H. G., Yang, D. S., & Kim, Y.-S. (2018). Assessing environmental flows of coordinated operation of dams and weirs in the Geum River basin under climate change scenarios. *Science of the Total Environment*, 643, 912–925. <https://doi.org/10.1016/j.scitotenv.2018.06.225>
- Palanichamy, A. (2013). Land use / land cover mapping in analysis of tiruchirappalli district, tamilnadu using geoinformatics. *International Journal of Latest Trends in Engineering and Technology*, 9(4), 161–165. <https://doi.org/10.21172/1.94.26>
- Alawamy, J. S., Balasundram, S. K., Mohd Hanif, A. H., & Boon Sung, C. T. (2020). Detecting and analysing land use and land cover changes in the region of Al-Jabal Al-Akhdar, Libya using time-series landsat data from 1985 to 2017. *Sustainability*, 12(11), 4490.
- Cesur, A., Cetin, I. Z., Cetin, M., Sevik, H., & Ozel, H. B. (2022). The use of Cupressus arizonica as a biomonitor of Li, Fe, and Cr pollution in Kastamonu. *Water Air Soil Pollut.*, 233, 193. <https://doi.org/10.1007/s11270-022-05667-w>. Vol.: (0123456789)1 3.
- Armstrong, A., Burton, R. R., Lee, S. E., Mobbs, S., Ostle, N., Smith, V., Waldron, S., & Whitaker, J. (2016). Ground-level climate at a peatland wind farm in Scotland is affected by wind turbine operation. *Environmental Research Letters*, 11, 044024.
- Arnell, N. W., & Gosling, S. N. (2013). The impacts of climate change on river flow regimes at the global scale. *Journal of Hydrology*, 486, 351–364.
- Atik, M., Altan, T., & Artar, M. (2010). Land use changes in relation to coastal tourism developments in Turkish Mediterranean. *Polish J Environ Stud*, 19(1), 21–33.
- Baessler, C., & Klotz, S. (2006). Effects of changes in agricultural land-use on landscape structure and arable weed vegetation over the last 50 years. *Agriculture, Ecosystems & Environment*, 115(1–4), 43–50. <https://doi.org/10.1016/j.agee.2005.12.007>

- Balachandar, D., Rutharvel Murthy, K., Muruganandam, R., Sumathi, M., & Sundararaj Kumaraswamy, K. (2011). Analysis of land use/land cover using remote sensing techniques a case study of Karur district, Tamil Nadu, India. *International Journal of Current Research*, 3(12), 226–229.
- Begum, R. A., Siwar, C., Abidin, R. D. Z. R. Z., & Pereira, J. J. (2011). Vulnerability of climate change and hardcore poverty in Malaysia. *Journal of Environmental Science and Technology*, 4(2), 112–117.
- Berhe, A. A., Arnold, C., Stacy, E., Lever, R., McCorkle, E., & Araya, S. N. (2014). Soil erosion controls on biogeochemical cycling of carbon and nitrogen. *Nature Education Knowledge*, 5(8), 2.
- Berihun, M. L., Tsunekawa, A., Haregeweyn, N., Meshesha, D. T., Adgo, E., Tsubo, M., ... & Yibeltal, M. (2019). Exploring land use/land cover changes, drivers and their implications in contrasting agro-ecological environments of Ethiopia. *Land Use Policy*, 87, 104052.
- Boavida-Portugal, I., Rocha, J., & Ferreira, C. C. (2016). Exploring the impacts of future tourism development on land use/cover changes. *Applied Geography*, 77, 82–91. <https://doi.org/10.1016/j.apgeog.2016.10.009>
- Börjesson, P., & Tufvesson, L. M. (2011). Agricultural crop-based biofuels—Resource efficiency and environmental performance including direct land use changes. *Journal of Cleaner Production*, 19(2–3), 108–120. <https://doi.org/10.1016/j.jclepro.2010.01.001>
- Bozdogan Sert, E., Turkmen, M., & Cetin, M. (2019). Heavy metal accumulation in rosemary leaves and stems exposed to traffic-related pollution near Adana-İskenderun Highway (Hatay, Turkey). *Environmental Monitoring and Assessment*, 191, 553. <https://doi.org/10.1007/s10661-019-7714-7>. <https://rd.springer.com/article/10.1007/s10661-019-7714-7>.
- Bozdogan Sert, E., Kaya, E., Adiguzel, F., Cetin, M., Gungor, S., Zeren Cetin, I., & Dinc, Y. (2021). Effect of the surface temperature of surface materials on thermal comfort: a case study of Iskenderun (Hatay, Turkey). *Theoretical and Applied Climatology*, 144(1), 103–113.
- Breiman, L. (2001). Using iterated bagging to debias regressions. *Machine Learning*, 45, 261–277.
- Caissie, D. (2006). The thermal regime of rivers: a review. *Freshwater Biology*, 51, 1389–1406. <https://doi.org/10.1111/j.1365-2427.2006.01597.x>
- Cetin, M., & Abo Aisha, A. E. S. (2023). Variation of Al concentrations depending on the growing environment in some indoor plants that used in architectural designs. *Environmental Science and Pollution Research*, 30(7), 18748–18754. <https://doi.org/10.1007/s11356-022-23434-6>. Access on 10 Jun 2023.
- Cetin, M., & Jawed, A. A. (2021). The chancing of Mg concentrations in some plants grown in Pakistan depends on plant species and the growing environment. *Kastamonu University Journal of Engineering and Sciences*, 7(2), 167–174.
- Cetin, M., & Jawed, A. A. (2022). Variation of Ba concentrations in some plants grown in Pakistan depending on traf density. *Biomass Conversion and Biorefinery*, 2022, 2023. <https://doi.org/10.1007/s13399-022-02334-2>. Accessed10Jun
- Cetin M. (2017). Change in amount of chlorophyll in some interior ornamental plants (Bazı İç Mekan Süs Bitkilerinde Klorofil Miktarının Değişimi) Kastamonu University. *Journal of Engineering and Sciences*, 3(1), 11–19. <https://doi.org/10.24214/jcbps.B.7.3.80717>
- Cetin, M. (2015). Using GIS analysis to assess urban green space in terms of accessibility: case study in Kutahya. *International Journal of Sustainable Development & World Ecology*, 22(5), 420–424. <https://doi.org/10.1080/13504509.2015.1061066>
- Cetin, M., & Sevik, H. (2016). Change of air quality in Kastamonu city in terms of particulate matter and CO2 amount. *Oxidation Communications*, 39(4), 3394–3401.
- Cetin, M., Isik Pekkan, O., Bilge Ozturk, G., et al. (2023). Determination of the impacts of mining activities on land cover and soil organic carbon: Altintepe Gold Mine Case, Turkey. *Water, Air, & Soil Pollution*, 234, 272. <https://doi.org/10.1007/s11270-023-06274-z>
- Chen, J., Wu, X., Finlayson, B. L., Webber, M., Wei, T., Li, M., & Chen, Z. (2014). Variability and trend in the hydrology of the Yangtze River, China: annual precipitation and runoff. *Journal of Hydrology*, 513, 403–412.
- Colins, W., Colman, R., Haywood, J., Manning, M. R., & Mote, P. (2007). The physical science behind climate change. *Scientific American*, 297, 62–73.
- Congalton, R. G. (1991a). A review of assessing the accuracy of classifications of remotely sensed data. *Remote Sensing of Environment*, 37(1), 35–46.
- Congalton, R. G. (1991b). Remote sensing and geographic information system data integration: error sources and. *Photogrammetric Engineering & Remote Sensing*, 57(6), 677–687.
- Costa, M. H., Botta, A., & Cardille, J. A. (2003). Effects of large-scale changes in land cover on the discharge of the Tocantins River, South-Eastern Amazonia. *Journal of Hydrology*, 283(1–4), 206–217.
- Crooks, S., Davies, H., & Goodsell, G. (2000). Rainfall runoff modelling and the impact of land use change in the Thams catchment. In *European Conference on Advances in Flood Research* (pp. 115–130). <https://www.researchgate.net/publication/295356271>
- DeFries, R., & Eshleman, K. N. (2004). Land-use change and hydrologic processes: a major focus for the future. *Hydrological Processes*, 18(11), 2183–2186.
- Dodds, W. K., Bouska, W. W., Eitzmann, J. L., Pilger, T. J., Pitts, K. L., Riley, A. J., ... & Thornbrugh, D. J. (2009). Eutrophication of US freshwaters: analysis of potential economic damages. *Environmental Science & Technology*, 43, 12–19. <https://doi.org/10.1021/es801217q> [PubMed] [Google Scholar]
- Döll, P., & Schmied, H. M. (2012). How is the impact of climate change on river flow regimes related to the impact on mean annual runoff? A global-scale analysis. *Environmental Research Letters*, 7(1), 014037. <https://doi.org/10.1088/1748-9326/7/1/014037>
- Döll, P., & Zhang, J. (2010). Impact of climate change on freshwater ecosystems: A global-scale analysis of ecologically relevant river flow alterations. *Hydrology and Earth System Sciences*, 14(5), 783–799. <https://doi.org/10.5194/hess-14-783-2010>

- Dong, R., Yu, L., & Liu, G. (2008). Impact of tourism development on landcover change in a matriarchal community in the Lugu Lake area. *The International Journal of Sustainable Development and World Ecology*, 15(1), 28–35. <https://doi.org/10.1080/13504500809469765>
- Dudgeon, D., Arthington, A., Gessner, M., Kawabata, Z.-I., Knowler, D., Lévêque, C., Naiman, R., Prieur-Richard, A.-H., Soto, D., Stiassny, M., & Sullivan, C. (2006). Freshwater biodiversity: Importance, threats, status and conservation challenges. *Biological Reviews of the Cambridge Philosophical Society*, 81, 163–182.
- Endo, H., Kodama, H., Fukuda, T., Sugimoto, T., & Horie, M. K. (2015). Effect of climatic conditions on energy consumption in direct fresh-air container data centers. *Sustainable Computing: Informatics and Systems*, 6, 17–25.
- Farfan, M. A., Vargas, J. M., Duarte, J., & Real, R. (2009). What is the impact of wind farms on birds? A case study in southern Spain. *Biodiversity and Conservation*, 18, 3743–3758. <https://doi.org/10.1007/s10531-009-9677-4>
- Fenta, A. A., Yasuda, H., Haregeweyn, N., Belay, A. S., Hadush, Z., Gebremedhin, M. A., & Mekonnen, G. (2017). The dynamics of urban expansion and land use/land cover changes using remote sensing and spatial metrics: the case of Mekelle City of northern Ethiopia. *International Journal of Remote Sensing*, 38(14), 4107–4129.
- Field, C. B., Barros, V., Stocker, T., Qin, D., Dokken, D., Ebi, K., Mastrandrea, M., Mach, K., Plattner, G., & Allen, S. (2012). IPCC, 2012: Managing the risks of extreme events and disasters to advance climate change adaptation. *A Special Report of Working Groups I and II of the Intergovernmental Panel on Climate Change*; Cambridge University Press: Cambridge, UK, 30, 7575–7613.
- Fohrer, N., Haverkamp, S., Eckhardt, K., & Frede, H. G. (2001). Hydrologic response to land use changes on the catchment scale. *Physics and Chemistry of the Earth, Part b: Hydrology, Oceans and Atmosphere*, 26(7–8), 577–582.
- Fugère, V., Nyboer, E. A., Bleecker, J. C., & Chapman, L. J. (2016). Impacts of forest loss on inland waters: Identifying critical research zones based on deforestation rates, aquatic ecosystem services, and past research effort. *Biological Conservation*, 201, 277–283. <https://doi.org/10.1016/j.biocon.2016.07.012>
- Futemma, C., & Brondizio, E. S. (2003). Land reform and land-use changes in the lower Amazon: Implications for agricultural intensification. *Human Ecology*, 31(3), 369–402. <https://doi.org/10.1023/A:1025067721480>
- Gashaw, T., Tulu, T., Argaw, M., & Worqlul, A. W. (2018). Modeling the hydrological impacts of land use/land cover changes in the Andassa watershed, Blue Nile Basin, Ethiopia. *Science of the Total Environment*, 619, 1394–1408.
- Geethalakshmi, V., & Dheebakaran, G. (2008). Impact of climate change on agriculture over Tamil Nadu. Chap IV. In G. S. L. H. V. Rao Prasad, G. G. S. N. Rao, V. U. M. Rao & Y. S. Ramakrishna (Eds.), *Climate change and agriculture over India* (pp. 80–93). CRIDA, Hyderabad. <https://www.researchgate.net/publication/286657821>
- Gernes, M. C., & Helgen, J. C. (2002). *Indexes of biological integrity (IBI) for large depressional wetlands in Minnesota*. Minnesota Pollution Control Agency, St. Paul, MN, USA.
- González-Villela, R., Martínez, M. J. M., & Sepúlveda, J. S. S. (2018). Effects of climate change on the environmental flows in the Conchos River (Chihuahua, Mexico). *Ecohydrology & Hydrobiology*, 18(4), 431–440. <https://doi.org/10.1016/j.ecohyd.2018.10.004>
- Gresselin, F., Dardaillon, B., Bordier, C., Parais, F., & Kauffmann, F. (2021). Use of statistical methods to characterize the influence of groundwater on the thermal regime of rivers in Normandy, France: Comparison between the highly permeable, chalk catchment of the Touques river and the low permeability, crystalline rock catchment of the Orne river. *Geological Society, London, Special Publications*, 517(1), 351–378. <https://doi.org/10.1144/SP517-2020-117>
- Gümüş, S., Bellibaş, M. Ş, Gümüş, E., & Hallinger, P. (2019). *Science mapping research on educational leadership and management in Turkey: A bibliometric review of international publications*. Advance online publication.
- Himika, S., & Kaur, R. (2018). Global land temperature prediction by machine learning combo approach. In: *2018 9th International Conference on Computing, Communication and Networking Technologies ICCCNT, 2018*, 1–8. <https://doi.org/10.1109/ICCCNT.2018.8494173>
- House, A. R., Thompson, J. R., Roberts, C., de Smeth, K., Old, G., & Acreman, M. C. (2017). Projecting impacts of climate change on habitat availability in a macrophyte dominated Chalk river. *Ecohydrology*, 10(4), e1823. <https://doi.org/10.1002/eco.1823>
- Indian Meteorological Department. (2001). IMD, Chennai. <https://mausam.imd.gov.in/Chennai>
- Isinkaralar, K., & Ramazan, E. (2021). Landscape plants as biomonitors for magnesium concentration in some species. *International Journal of Progressive Sciences and Technologies*, 29(2), 468–473.
- İşınkaralar, Ö., & Varol, Ç. (2021). Kent merkezlerinde ticaret birimlerin mekansal örüntüsü üzerine bir değerlendirme: kastamonu örneği. *Journal of Architectural Sciences and Applications*, 6(2), 396–403. <https://doi.org/10.30785/mbud.927529>
- Iyappan, L., & Maria Subashini, L. (2014). Landuse change detection in Namakkal Taluk using remote sensing. *International Journal of Applied Engineering Research*, 9(22), 5699–5707. ISBN 0973-4562.
- Karl, T. R. (1998). Regional trends and variations of temperature and precipitation. *The Regional Impacts of Climate Change: an Assessment of Vulnerability*, 411, 425.
- Kilicoglu, C., Cetin, M., Aricak, B., & Sevik, H. (2021). Integrating multicriteria decision-making analysis for a GIS-based settlement area in the district of Atakum, Samsun Turkey. *Theoretical and Applied Climatology*, 143, 379–388. <https://doi.org/10.1007/s00704-020-03439-2>
- Klink, C. A., Moreira, A. G., & Solbrig, O. T. (1993). Ecological impacts of agricultural development in the Brazilian Cerrados. In M. D. Young & O. T. Solbrig (Eds.), *The World's Savannas: economic driving forces, ecological constraints and policy options for sustainable land use (Man in the Biosphere Series 12* (pp. 259–283). Parthenon Publishing.

- Korkanç, S. Y., Şahin, H., Özden, A. O., & Özkurt, B. (2018). The effects of land use transformations on organic carbon storage and some properties of soils: The case of Niğde region. *Turkey Forestry Journal*, 19(4), 362–367.
- Krishna Kumar, K., Patwardhan, S. K., Kulkarni, A., Kamala, K., Rao, K. K., & Jones, R. (2011). Simulated projections for summer monsoon climate over India by a high-resolution regional climate model (PRECIS). *Current Science*, 101, 312–326.
- Laizé, C. L. R., Acreman, M. C., Schneider, C., Dunbar, M. J., Houghton-Carr, H. A., Flörke, M., & Hannah, D. M. (2014). Projected flow alteration and ecological risk for pan-European rivers. *River Research and Applications*, 30(3), 299–314. <https://doi.org/10.1002/rra.2645>
- Lal, R. (2003). Soil erosion and the global carbon budget. *Environment International*, 29(4), 437–450.
- Lal, R. (2004). Soil carbon sequestration impacts on global climate change and food security. *Science*, 304(5677), 1623–1627.
- Lambin, E. F., Geist, H. J., & Lepers, E. (2003). Dynamics of land-use and land-cover change in tropical regions. *Annual Review of Environment and Resources*, 28(1), 205–241.
- Lillesand, T., Kiefer, R. W., & Chipman, J. (2015). *Remote sensing and image interpretation*. John Wiley & Sons.
- Liu, H., Zhang, S., Li, Z., Lu, X., & Yang, Q. (2004). Impacts on wetlands of largescale land-use changes by agricultural development: the small Sanjiang plain, China. *AMBIO: A Journal of the Human Environment*, 33(6), 306–310.
- Lu, Y., Wu, P., Ma, X., & Li, X. (2019). Detection and prediction of land use/land cover change using spatiotemporal data fusion and the Cellular Automata–Markov model. *Environmental Monitoring and Assessment*, 191(2), 1–19.
- Maia, S. M. F., Ogle, S. M., Cerri, C. C., & Cerri, C. E. P. (2010). Changes in soil organic carbon storage under different agricultural management systems in the Southwest Amazon Region of Brazil. *Soil Till Research*, 106, 177–184.
- Mao, X., Meng, J., & Wang, Q. (2014). Modeling the effects of tourism and land regulation on land-use change in tourist regions: aA case study of the Lijiang River Basin in Guilin, China. *Land Use Policy*, 41, 368–377. <https://doi.org/10.1016/j.landusepol.2014.06.018>
- Mao, D., & Cherkauer, K. A. (2009). Impacts of land-use change on hydrologic responses in the Great Lake region. *Journal Hydrology*, 374(71–82). <https://doi.org/10.1016/j.jhydrol.2009.06.016>.
- Marvel, K., & Bonfils, C. (2013). Identifying external influences on global precipitation. *Proceedings of the National Academy of Sciences USA*, 110(48), 19301–19306.
- Meer, M. S., & Mishra, A. K. (2020). Land use/land cover changes over a district in northern India using remote sensing and GIS and their impact on society. and environment. *Journal of the Geological Society of India*, 95, 179–182.
- Cetin, M., Aljama, A. M. O., Alrabiti, O. B. M., Adiguzel, F., Sevik, H., & Cetin, I. Z. (2022). Determination and mapping of regional change of Pb and Cr pollution in Ankara City Center. *Water, Air, & Soil Pollution*, 233, 163. <https://doi.org/10.1007/s11270-022-05638-1>
- Meshesha, D. T., Tsunekawa, A., & Tsubo, M. (2012). Continuing land degradation: Cause–effect in Ethiopia’s Central Rift Valley. *Land Degradation & Development*, 143, 130–143. <https://doi.org/10.1002/ldr.1061>
- Meshesha, D. T., Tsunekawa, A., Tsubo, M., Ali, S. A., & Haregeweyn, N. (2014). Land-use change and its socio-environmental impact in Eastern Ethiopia’s highland. *Regional Environmental Change*, 14, 757–768.
- Mohseni, O., & Stefan, H. G. (1999). Stream temperature/air temperature relationship: a physical interpretation. *Journal of Hydrology*, 218, 128–141.
- Moravec, D., Barták, V., Puš, V., & Wild, J. (2018). Wind turbine impact on near-ground air temperature. *Renew Energy*, 123, 627–633.
- Morello, L., Abbott, A., & Butler, D. (2014). 365days:2014 in science. *Nature*, 516, 300–303.
- Norman, J. M., & Becker, F. (1995). Terminology in thermal infrared remote sensing of natural surfaces. *Agricultural and Forest Meteorology*, 77(3–4), 153–166. [https://doi.org/10.1016/0168-1923\(95\)02259-z](https://doi.org/10.1016/0168-1923(95)02259-z)
- Ozturk, S., & Isinkaralar, O. (2019). Parking Problematique in Kastamonu City Center: a critical evaluation. *The Journal of International Social Research*, 12(67), 506–511.
- Öztürk, S., Işınkaralar, Ö., Yılmaz, D., Şimşek, M., Almansouri, H. M. S., & Elahsadi, A. H. M. (2021). Covid19’un tüketici alışkanlıklarına etkisi üzerine bir araştırma: Türkiye-Libya karşılaştırması. *Doğu Coğrafya Dergisi*, 26(46), 97–108. <https://doi.org/10.17295/ataunidcd.958864>
- Pastor, A. V., Palazzo, A., Havlik, P., Biemans, H., Wada, Y., Obersteiner, M., et al. (2019). The global nexus of food–trade–water sustaining environmental flows by 2050. *Nature Sustainability*, 2, 499–507. <https://doi.org/10.1038/s41893-019-0287-1>
- Pazúr, R., & Bolliger, J. (2017). Land changes in Slovakia: Past processes and future directions. *Applied Geography*, 85, 163–175.
- Piao, S. L., Ciais, P., Huang, Y., Shen, Z. H., Peng, S. S., Li, J. S., Zhou, L. P., Liu, H. Y., Ding, Y. H., Pingale, S. M., Khare, D., Jat, M. K., & Adamowski, J. (2014). Spatial and temporal trends of mean and extreme rainfall and temperature for the 33 urban centers of the arid and semi-arid state of Rajasthan, India. *Atmospheric Research*, 138, 73–90.
- Pimentel, D., Zuniga, R., & Morrison, D. (2005). Update on the environmental and economic costs associated with alien-invasive species in the United States. *Ecological Economics*, 52, 273–288.
- Bal, P. K., Ramachandran, A., Geetha, R., Bhaskaran, B., Thirumurugan, P., Indumathi, J., & Jayanthi, N. (2016). Climate change projections for Tamil Nadu: Deriving high resolution climate data by a downscaling approach using PRECIS. *Theoretical and Applied Climatology*, 123, 523–535. <https://doi.org/10.1007/s00704-014-1367-9>
- Qin, X., Sun, J., & Wang, X. (2018). Plant coverage is more sensitive than species diversity in indicating the dynamics of the above-ground biomass along a precipitation gradient on the Tibetan Plateau. *Ecological Indicators*, 84, 507–514.

- Rajewski, D. A., Takle, E. S., VanLoocke, A., & Purdy, S. L. (2020). Observations show that wind farms substantially modify the atmospheric boundary layer thermal stratification transition in the early evening. *Geophysical Research Letters*, *47*, e2019GL086010.
- Ravichandran, S., & Manonmani, I. K. (2021). Land use – land cover change analysis of Karur Town – A GIS approach. *International Journal of Scientific Research in Science and Technology* Print ISSN: 2395–6011 | Online ISSN: 2395–602X (www.ijrst.com) <https://doi.org/10.32628/IJSRST218373>.
- Rientjes, T., Haile, A., Kebede, E., Mannaerts, C. M. M., Habib, E., Steenhuis, T. S. (2011). Changes in land cover, rainfall and streamflow in Upper GilgelAbbay catchment, Blue Nile basin, Ethiopia. *Hydrology and Earth System Sciences*, *15*, 1979–1989. <https://doi.org/10.5194/hess-15-1979-2011>
- Rose, S., & Peters, N. E. (2001). Effects of urbanization on streamflow in the Atlanta area (Georgia, USA): a comparative hydrological approach. *Hydrological Processes*, *15*(8), 1441–1457.
- Salmoral, G., Willaarts, B. A., Troch, P. A., & Garrido, A. (2015). Drivers influencing streamflow changes in the Upper Turia basin, Spain. *Science of the Total Environment*, *503*, 258–268.
- Scanlon, B. R., Jolly, I. D., Sophocleous, M., & Zhang, L. (2006). Global impacts of agricultural land-use changes on water resources: Quantity versus quality. *Water Resources Research*. <https://doi.org/10.1029/2006WR005486>
- Scharlemann, J. P., Tanner, E. V., Hiederer, R., & Kapos, V. (2014). Global soil carbon: understanding and managing the largest terrestrial carbon pool. *Carbon Manage.*, *5*(1), 81–91.
- Setegn, S. G., Srinivasan, R., & Dargahi, B. (2008). Hydrological modelling in the Lake Tana Basin, Ethiopia using SWAT model. *The Open Hydrology Journal*, *2*(1). <https://doi.org/10.2174/1874378100802010049>
- Shahid, M., Dumat, C., Khalid, S., Schreck, E., Xiong, T., & Niazi, N. K. (2017). Foliar heavy metal uptake, toxicity and detoxification in plants: a comparison of foliar and root metal uptake. *Journal of Hazardous Materials*, *325*, 36–58.
- Silberstein, R. P., Aryal, S. K., Durrant, J., Pearcey, M., Braccina, M., Charles, S. P., ... & McFarlane, D. J. (2012). Climate change and runoff in south-western Australia. *Journal of Hydrology*, *475*, 441–455.
- Şimşek, Ç. K., Türk, T., Ödül, H., & Çelik, M. N. (2018). Detection of paragliding fields by GIS. *International Journal of Engineering and Geosciences*, *3*(3), 119–125. <https://doi.org/10.26833/ijeg.413833>
- Sinokrot, B. A., & Gulliver, J. S. (2000). In-stream flow impact on river water temperatures. *Journal of Hydraulic Research*, *38*(5), 339–349. <https://doi.org/10.1080/00221680009498315>
- Smith, T. F., Carter, R. W., Daffara, P., & Keys, N. (2010). The nature and utility of adaptive capacity research. National Climate Change Adaptation Research Facility (NCCARF), Griffith University, Gold Coast Campus, Southport, Australia, p 68
- Song, X. P., Hansen, M. C., Stehman, S. V., Potapov, P. V., Tyukavina, A., Vermote, E. F., & Townshend, J. R. (2018). Global land change from 1982 to 2016. *Nature*, *560*, 639–643. [https://doi.org/10.5937/GeoPan1602105S](https://doi.org/10.1038/s41586-018-0411-Srinivasan, R., Zhang, X., & Arnold, J. (2010). SWAT ungauged: Hydrological budget and crop yield predictions in the Upper Mississippi River Basin. <i>Transactions of the ASABE</i>, <i>53</i>(5), 1533–1546.</i></p>
<p>Stankov U, Klaučo M, Dragičević V, Vujičić MD, Solarević M. (2016). Assessing land-use changes in tourism area on the example of Čajetina municipality (Serbia). <i>Geographica Pannonica</i>, <i>20</i>(2), 105– 113. <a href=)
- Suvetha, M., & Maniyosai, R. (2018). An analytical study on agricultural activities in Karur district and the temperament of agriculturists. *Journal of Emerging Technologies and Innovative Research (JETIR)*, *5*(12). <https://www.jetir.org>
- Tabari, H., & Willems, P. (2018). More prolonged droughts by the end of the century in the Middle East. *Environmental Research Letters*, *13*(10), 104005.
- Tağıl, Ş., & Ersayın, K. (2015). Balıkesir İlinde Dış Ortam Termal Konfor Değerlendirmesi. *The Journal of International Social Research*, *8*(41). *Yuka and Toroğlu*, *7*(2), 155–166.
- Tan, K. C., San Lim, H., MatJafri, M. Z., & Abdullah, K. (2010). Landsat data to evaluate urban expansion and determine land use/land cover changes in Penang Island, Malaysia. *Environmental Earth Sciences*, *60*(7), 1509–1521. <https://doi.org/10.1007/s12665-009-0286-z>
- Thompson, J. R., Irvani, H., Clilverd, H. M., Sayer, C. D., Heppell, C. M., & Axmacher, J. C. (2017). Simulation of the hydrological impacts of climate change on a restored floodplain. *Hydrological Sciences Journal*, *62*(15), 2482–2510. <https://doi.org/10.1080/02626667.2017.1390316>
- Thompson, J. R., Laizé, C. L. R., Acreman, M. C., Crawley, A., & Kingston, D. G. (2021). Impacts of climate change on environmental flows in West Africa’s Upper Niger Basin and the Inner Niger Delta. *Hydrology Research*, *52*(4), 958–974.
- Tickner, D., Opperman, J. J., Abell, R., Acreman, M. C., Arthington, A. H., Bunn, S. E., et al. (2020). Bending the curve of global freshwater biodiversity loss: an emergency recovery plan. *BioScience*, *70*(4), 330–342. <https://doi.org/10.1093/biosci/biaa002>
- Trenberth, K. E. (2015). Has there been a hiatus? *Science*, *349*, 691–692.
- Twisa, S., & Buchroithner, M. F. (2019). Land-use and land-cover (LULC) change detection in Wami River Basin, Tanzania. *Land*, *8*(9), 136.
- Unique Identification Authority of India (UIDAI). (2023). <https://myaadhaar.uidai.gov.in>
- Van Vliet, M. T. H., Franssen, W. H. P., Yearsley, J. R., Ludwig, F., Haddeland, I., Lettenmaier, D. P., & Kabat, P. (2013). Global river discharge and water temperature under climate change. *Global Environmental Change*, *23*, 450–464.
- Veldkamp, T. I. E., Zhao, F., Ward, P. J., de Moel, H., Aerts, J. C. J. H., Schmied, H. M., et al. (2018). Human impact parameterizations in global hydrological models improve estimates of monthly discharges and hydrological extremes: a multi-model validation study. *Environmental*

- Research Letters*, 13(5), 055008. <https://doi.org/10.1088/1748-9326/aab96f>
- Vitousek, P. M., Mooney, H. A., Lubchenco, J., & Melillo, J. M. (1997). Human domination of earth's ecosystems. *Science*, 277, 494–499. <https://doi.org/10.1126/science.277.5325.494>
- Vorismarty, C. J., Green, P., Salisbury, J., & Lammers, R. B. (2000). Global water resources: Vulnerability from climate change and population growth. *Science*, 289(5477), 284–288.
- Vörösmarty, C. J., McIntyre, P. B., Gessner, M. O., Dudgeon, D., Prusevich, A., Green, P., et al. (2010). Global threats to human water security and river biodiversity. *Nature*, 467, 555–561. <https://doi.org/10.1038/nature09440>
- Walsh, M. E., Daniel, G., Shapouri, H., & Slinsky, S. P. (2003). Bioenergy crop production in the United States: potential quantities, land use changes, and economic impacts on the agricultural sector. *Environmental and Resource Economics*, 24(4), 313–333. <https://doi.org/10.1023/A:1023625519092>
- Wang, J. M., Zhang, J. R., & Feng, Y. (2019). Characterizing the spatial variability of soil particle size distribution in an underground coal mining area: an approach combining multi-fractal theory and geostatistics. *CATENA*, 176, 94–103.
- Wang, Y., Xu, Y., Lei, C., Li, G., Han, L., Song, S., ... & Deng, X. (2016). Spatio-temporal characteristics of precipitation and dryness/wetness in Yangtze River Delta, eastern China, during 1960–2012. *Atmospheric Research*, 172, 196–205.
- Warburton, M. L., Schulze, R. E., & Jewitt, G. P. (2012). Hydrological impacts of land use change in three diverse South African catchments. *Journal of Hydrology*, 414, 118–135.
- Webb, B. W., Clack, P. D., & Walling, D. E. (2003). Water–air temperature relationships in a Devon river system and the role of flow. *Hydrological Processes*, 17, 3069–3084.
- Woodward, G., Perkins, D. M., & Brown, L. E. (2010). Climate change and freshwater ecosystems: Impacts across multiple levels of organization. *Philosophical Transactions of the Royal Society of London. Series b, Biological Sciences*, 365, 2093–2106.
- Xi, J., Zhao, M., Ge, Q., & Kong, Q. (2014). Changes in land use of a village driven by over 25 years of tourism: the case of Gougezhuang village, China. *Land Use Policy*, 40, 119–130.
- Xia, G., Zhou, L., Freedman, J. M., Roy, S. B., Harris, R. A., & Cervarich, M. C. (2016). A case study of effects of atmospheric boundary layer turbulence, wind speed, and stability on wind farm induced temperature changes using observations from a field campaign. *Climate Dynamics*, 46, 2179–2196.
- Yu, M., Li, Q., Hayes, M. J., Svoboda, M. D., & Heim, R. R. (2014). Are droughts becoming more frequent or severe in China based on the standardized precipitation evapotranspiration index: 1951–2010. *International Journal of Climatology*, 34(3), 545–558.
- Zhang, H., Jin, G., & Yu, Y. (2018). Review of river basin water resource management in China. *Water*, 10(4), 425.
- Zhou, L., Tian, Y., Baidya Roy, S., Thorncroft, C., Bosart, L. F. & Hu, Y. (2012). Impacts of wind farms on land surface temperature. *Nature Climate Change*. <https://doi.org/10.1038/nclimate1505>
- Adiguzel, F., Bozdogan Sert, E., Dinc, Y., Cetin, M., Gungor, S., Yuka, P., ... & Vural, E. (2022). Determining the relationships between climatic elements and thermal comfort and tourism activities using the tourism climate index for urban planning: a case study of Izmir Province. *Theoretical and Applied Climatology*, 147(3), 1105–1120.

Publisher's Note Springer Nature remains neutral with regard to jurisdictional claims in published maps and institutional affiliations.

Springer Nature or its licensor (e.g. a society or other partner) holds exclusive rights to this article under a publishing agreement with the author(s) or other rightsholder(s); author self-archiving of the accepted manuscript version of this article is solely governed by the terms of such publishing agreement and applicable law.